Mononuclear Organometallic Platinum(II) Complexes and Platinum(II)−Copper(I) Mixed Complexes from Symmetrical 3,5-Bis(iminoacetyl)pyrazolate Ligands

Marc-Etienne Moret and Peter Chen*

Labor für Organische Chemie, ETH Zürich, CH-8093 Zürich, Switzerland

Received May 6, 2008

The reaction of symmetrical dinucleating ligands 3,5-bis(4-methoxyphenyliminoacetyl)-4-methylpyrazole (bmimpH, **1a**) and 3,5-bis(2,6-dimethylphenyliminoacetyl)-4-methylpyrazole (bdmimpH, **1b**) with $[(\mu\text{-}Me_2S)PtMe_2]_2$ or $(Me_2S)_2PtPh_2$ affords selectively mononuclear complexes $LPtMe(SMe_2)$ or $LPtPh(SMe_2)$ (L = bmimp, bdmimp). Reaction of these complexes with CuCl gives access to ionic compounds $\{[LPtMe(SMe_2)]_2Cu^+CuCl_2^-$ and $[LPtPh(SMe_2)]_2Cu^+CuCl_2^-$, which exhibit dynamic behavior in solution for L = bdmimp. Ligand deprotonation followed by reaction with $(Me_2S)_2PtPh_2$ affords mononuclear anionic complexes $K^+[LPtPh_2]^-$. These react with CuCl to give dimeric structures of formula $\{[LPtPh_2]_2Cu_2\}$, which exhibit Pt→Cu dative bonds and a Cu−Cu contact, and dynamic behavior in solution.

Introduction

The selective activation and functionalization of alkyl and aryl C−H bonds under mild conditions is a major challenge for today's chemists.[1−4] The versatile chemistry of transition metals, which are able to bind to alkanes and arenes and form strong M−C and M−H bonds, is likely to play an important role in this field. As a matter of fact, C−H bond activation has been observed for a range of different transition metals.[5−19] In particular, organometallic complexes of platinum incorporating N-donor ligands have been shown to activate the C−H bonds of benzene[20−27] and methane[28−31] to form phenyl or methyl complexes, respectively. Higher alkanes can also be activated to give dehydrogenation products.[32−34] The mechanism of some of these transformations has been extensively studied by several groups,[21,23,29,30,32−45] including ours.[46−49] These reactions are thought to proceed through the initial complexation of a σ C−H

* Corresponding author. E-mail: chen@org.chem.ethz.ch.

(1) Labinger, J. A.; Bercaw, J. E. *Nature* **2002**, *417*, 507–514.
(2) Periana, R. A.; Bhalla, G.; Tenn III, W. J.; Young, K. J. H.; Liu, X. Y.; Mironov, O.; Jones, C. J.; Ziatdinov, V. R. *J. Mol. Catal. A* **2004**, *220*, 7–25.
(3) Labinger, J. A. *J. Mol. Catal. A* **2004**, *220*, 27–35.
(4) Bergman, R. G. *Nature* **2007**, *446*, 391–393.
(5) Kawashima, T.; Takao, T.; Suzuki, H. *J. Am. Chem. Soc.* **2007**, *129*, 11006–11007.
(6) Kirillova, M. V.; Kuznetsov, M. L.; Reis, P. M.; da.Silva, J. A. L.; da.Silva, J. J. R. F.; Pombeiro, A. J. L. *J. Am. Chem. Soc.* **2006**, *129*, 10531–10545.
(7) Kuninobu, Y.; Nishina, Y.; Takeuchi, T.; Takai, K. *Angew. Chem., Int. Ed.* **2007**, *46*, 6518–6520.
(8) Wasserscheid, P.; Weiss, T.; Agel, F.; Werth, C.; Jess, A.; Forster, R. *Angew. Chem., Int. Ed.* **2007**, *46*, 46.
(9) Periana, R. A.; Mironov, O.; Taube, D.; Bhalla, G.; Jones, C. J. *Science* **2003**, *301*, 814–818.
(10) Hull, K. L.; Sanford, M. S. *J. Am. Chem. Soc.* **2007**, *129*, 11904–11905.
(11) Chen, M. S.; White, M. C. *Science* **2007**, *318*, 783–787.
(12) Tsang, J. Y. K.; Buschhaus, M. S. A.; Legzdins, P. *J. Am. Chem. Soc.* **2007**, *129*, 5372–5373.
(13) Blackmore, I. J.; Semiao, C. J.; Buschhaus, M. S. A.; Patrick, B. O.; Legzdins, P. *Organometallics* **2007**, *26*, 4881–4889.
(14) Kloek, S. M.; Heinekey, D. M.; Goldberg, K. I. *Angew. Chem., Int. Ed.* **2007**, *46*, 4736–4738.
(15) Herrerías, C. H.; Yao, X.; Li, Z.; Li, C.-J. *Chem. Rev.* **2006**, *107*, 2546–2562.
(16) Leung, C. W.; Zheng, W.; Wang, D.; Ng, S. M.; Yeung, C. H.; Zhou, Z.; Lin, Z.; Lau, C. P. *Organometallics* **2007**, *26*, 1924–1933.
(17) Shilov, A. E.; Shul'pin, G. B. *Chem. Rev.* **1997**, *97*, 2879–2932.
(18) Liang, L.-C.; Chien, P.-S.; Huang, Y.-L. *J. Am. Chem. Soc.* **2006**, *128*, 15562–15563.
(19) Lafrance, M.; Fagnou, K. *J. Am. Chem. Soc.* **2006**, *128*, 16496–16497.
(20) Garnett, J. L.; Hodges, R. J. *J. Am. Chem. Soc.* **1967**, *89*, 4546–4547.
(21) Iverson, C. N.; Carter, C. A. G.; Baker, R. T.; Scollard, J. D.; Labinger, J. A.; Bercaw, J. E. *J. Am. Chem. Soc.* **2003**, *125*, 12674–12675.
(22) Perdew, J. P.; Burke, K.; Wang, Y. *Phys. Rev. B* **1996**, *54*, 16533.
(23) Reinartz, S.; White, P. S.; Brookhart, M.; Templeton, J. L. *J. Am. Chem. Soc.* **2001**, *123*, 12724–12725.
(24) Zhang, F.; Kirby, C. W.; Hairsine, D. W.; Jennings, M. C.; Puddephatt, R. J. *J. Am. Chem. Soc.* **2005**, *127*, 14196–14197.
(25) Young, K. J. H.; Meier, S. K.; Gonzales, J. M.; Oxgaard, J.; Goddard III, W. A.; Periana, R. A. *Organometallics* **2006**, *25*, 4734–4737.
(26) Khaskin, E.; Zavalij, P. Y.; Vedernikov, A. N. *J. Am. Chem. Soc.* **2006**, *128*, 13054–13055.
(27) Karshtedt, D.; McBee, J. L.; Bell, A. T.; Tilley, T. D. *Organometallics* **2006**, *25*, 1801–1811.
(28) Periana, R. A.; Taube, D. J.; Gamble, S.; Taube, H.; Satoh, T.; Fujii, H. *Science* **1998**, *280*, 560–564.
(29) Lo, H. C.; Haskel, A.; Kapon, M.; Keinan, E. *J. Am. Chem. Soc.* **2002**, *124*, 3226–3228.
(30) Wick, D. D.; Goldberg, K. I. *J. Am. Chem. Soc.* **1997**, *119*, 10235–10236.
(31) Johannsson, L.; Ryan, O. B.; Tilset, M. *J. Am. Chem. Soc.* **1999**, *121*, 1974–1975.
(32) Kostelansky, C. N.; MacDonald, M. G.; White, P. S.; Templeton, J. L. *Organometallics* **2006**, *25*, 2993–2998.
(33) Khaskin, E.; Zavalij, P. Y.; Vedernikov, A. N. *J. Am. Chem. Soc.* **2006**, *128*, 13054–13055.
(34) Chen, G. S.; Labinger, J. A.; Bercaw, J. E. *Proc. Natl. Acad. Sci. U.S.A.* **2007**, *104*, 6915–6920.
(35) Lersch, M.; Tilset, M. *Chem. Rev.* **2005**, *105*, 2471–2526.
(36) Johansson, L.; Tilset, M.; Labinger, J. A.; Bercaw, J. E. *J. Am. Chem. Soc.* **2000**, *122*, 10846–10855.
(37) Zhong, H. A.; Labinger, J. A.; Bercaw, J. E. *J. Am. Chem. Soc.* **2002**, *124*, 1378–1399.
(38) Procelewska, J.; Zahl, A.; van Eldik, R.; Labinger, J. A.; Bercaw, J. E. *Inorg. Chem.* **2002**, *41*, 2808–2810.
(39) Driver, T. G.; Day, M. W.; Labinger, J. A.; Bercaw, J. E. *Organometallics* **2005**, *24*, 3644–3654.
(40) Owen, J. S.; Labinger, J. A.; Bercaw, J. E. *J. Am. Chem. Soc.* **2006**, *128*, 2005–2016.
(41) Johansson, L.; Ryan, O. B.; Rømming, C.; Tilset, M. *J. Am. Chem. Soc.* **2001**, *123*, 6579–6590.

10.1021/om800403y CCC: $40.75
Publication on Web 09/03/2008

bond to a Pt(II) center, followed by oxidative addition to form a transient Pt(IV) phenyl (or alkyl) hydride complex. Ligand exchange is often rate determining.

In most cases though, the formed phenyl or methyl complexes do not undergo the subsequent reactions that would be required for achieving an efficient catalytic transformation of benzene or methane. The most noticeable exception is the Catalytica system,[28] which is able to convert methane into methyl sulfate using a N−N chelated Pt catalyst in hot sulfuric acid. Several cases of catalytic hydroarylation of alkenes[27,50−52] using related complexes have also been reported.

One possibility to tune the reactivity of a metal center is to make use of cooperative effects in bimetallic complexes,[53,54] which can result in alteration of the redox behavior of the metal centers[55] or in a variety of reaction pathways allowed by the coordination of the substrate(s) to multiple metal centers.[56] Copper has found many uses in catalytic redox chemistry, due to fast ligand exchange and the accessibility of three oxidation states in solution, as well as to its ability to activate dioxygen. Of particular interest is the recent development of Cu-catalyzed aromatic oxidative coupling[57−60] based on the century-old Ullmann chemistry. In an attempt to couple platinum and copper activities, Tilley et al.[61] recently reported the preparation of bimetallic Pt−Cu complexes using a dinucleating PPNN ligand, where the platinum(II) center is chelated by two phosphorus atoms and the copper(I) by two nitrogen atoms. We aim at the preparation of Pt−Cu complexes with *all*-N dinucleating ligands, which may open access to new reactivity based on C−H activation by N-coordinated platinum(II).

The synthesis of well-defined bimetallic complexes in a controlled way requires the use of dinucleating ligands, which generally consist of a bridging unit attached on each side to one or more chelating arms.[62] Ligands incorporating pyrazolate as a bridging unit have been used to produce a wide range of bi- and polymetallic structures.[63−69] Symmetrical dinucleating ligands have the advantage of being synthetically easily accessible, but often require well-controlled successive introduction of both metals, as the binding sites are identical.[64,70] The readily available, symmetrical bis(iminoacetyl)pyrazolate ligands have been recently used to prepare homobimetallic palladium and nickel complexes for olefin polymerization.[71,72] As diimine chelating ligands would be suitable for both platinum and copper, we investigated the possibility of using this class of ligands for the preparation of platinum-containing heterobimetallic complexes.

In this work, we used two different approaches to prepare and characterize mononuclear organometallic platinum(II) complexes of symmetrical bis(iminoacetyl)pyrazolate. In the first strategy, we exploited a stoichiometric activation of the pyrazole N−H bond by platinum, while the second one relied on the steric bulk of phenyl ligands. The targeted mononuclear platinum(II) complexes were selectively obtained in both cases, and their coordination to copper(I) was studied using NMR, electrospray ionization mass spectrometry (ESI-MS), and X-ray crystallography.

Scheme 1.[a]

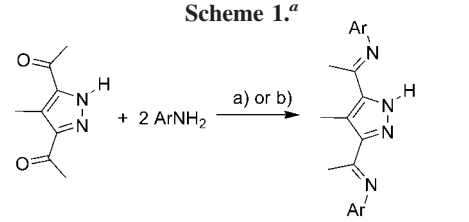

1a: Ar = *p*-$MeOC_6H_4$
1b: Ar = 2,6-$Me_2C_6H_4$

[a] Reaction conditions: a) Ar = *p*-methoxyphenyl, cat. HCOOH, MeOH, room temperature, 77%; b) Ar = 2,6-dimethylphenyl, cat. TsOH, toluene, Δ, 78%.

Results and Discussion

Ligand Synthesis. 3,5-Bis(4-methoxyphenyliminoacetyl)-4-methylpyrazole (bmimpH, **1a**) could be conveniently synthesized in good yield by imine condensation of 3,5-diacetyl-4-methylpyrazole and *p*-methoxyaniline in methanol at room temperature, using formic acid as a catalyst (see Scheme 1). The more bulky 2,6-dimethylaniline did not react under the same conditions. However, using the conditions of Noël et al.[64] (refluxing toluene, *p*-toluenesulfonic acid catalyst), 3,5-bis(2,6-dimethylphenyliminoacetyl)-4-methylpyrazole (bdmimpH, **1b**) could be prepared in good yield.

N−H Activation Based Strategy. As the pyrazole bridging unit of ligands **1a**,**b** have one acidic proton, we reasoned that a complex formation reaction that involves a stoichiometric reaction of the labile N−H bond should selectively afford

(42) Wik, B. J.; Lersch, M.; Krivokapic, A.; Tilset, M. *J. Am. Chem. Soc.* **2006**, *128*, 2682–2696.
(43) Heiberg, H.; Johansson, L.; Gropen, O.; Ryan, O. B.; Swang, O.; Tilset, M. *J. Am. Chem. Soc.* **2000**, *122*, 10831–10845.
(44) Hill, G. S.; Puddephatt, R. J. *Organometallics* **1998**, *17*, 1478–1486.
(45) Paul, A.; Musgrave, C. B. *Organometallics* **2007**, *26*, 793–809.
(46) Hammad, L. A.; Gerdes, G.; Chen, P. *Organometallics* **2005**, *24*, 1907–1913.
(47) Gerdes, G.; Chen, P. *Organometallics* **2004**, *23*, 3031–3036.
(48) Gerdes, G.; Chen, P. *Organometallics* **2003**, *22*, 2217–2225.
(49) Moret, M.-E.; Chen, P. *Organometallics* **2007**, *26*, 1523–1530.
(50) Karshtedt, D.; Bell, A. T.; Tilley, T. D. *Organometallics* **2004**, *23*, 4169–4171.
(51) Liu, C.; Han, X.; Wang, X.; Widenhoefer, R. A. *J. Am. Chem. Soc.* **2004**, *126*, 3700–3701.
(52) Han, X.; Widenhoefer, R. A. *Org. Lett.* **2006**, *8*, 3801–3804.
(53) van den Beuken, E. K.; Feringa, B. L. *Tetrahedron* **1998**, *54*, 12985–13011.
(54) Wheatley, N.; Kalck, P. *Chem. Rev.* **1999**, *99*, 3379–3419.
(55) Bosnich, B. *Inorg. Chem.* **1999**, *38*, 2554–2562.
(56) Ritleng, V.; Chetcuti, M. J. *Chem. Rev.* **2007**, *107*, 797–858.
(57) Chan, D. M. T.; Monaco, K. L.; Wand, R.-P.; Winters, M. P. *Tetrahedron Lett.* **1998**, *39*, 2933–2936.
(58) Temma, T.; Hatano, B.; Habaue, S. *Tetrahedron* **2006**, *62*, 8559–8563.
(59) Collman, J. P.; Zhong, M.; Zhang, C.; Costanzo, S. *J. Org. Chem.* **2001**, *66*, 7892–7897.
(60) Collman, J. P.; Zhong, M. *Org. Lett.* **2000**, *2*, 1233–1236.
(61) Karshtedt, D.; Bell, A. T.; Tilley, T. D. *Organometallics* **2003**, *22*, 2855–2861.
(62) Gavrilova, A. L.; Bosnich, B. *Chem. Rev.* **2004**, *104*, 349–383.
(63) Dubs, C.; Inagaki, A.; Akita, M. *Chem. Commun.* **2004**, 2760–2761.
(64) Dubs, C.; Yamamoto, T.; Inagaki, A.; Akita, M. *Organometallics* **2006**, *25*, 1344–1358.
(65) Dubs, C.; Yamamoto, T.; Inagaki, A.; Akita, M. *Organometallics* **2006**, *25*, 1359–1367.
(66) Schenk, T. G.; Downes, J. M.; Milne, C. R. C.; MacKenzie, P. B.; Boucher, H.; Whelan, J.; Bosnich, B. *Inorg. Chem.* **1985**, *24*, 2334–2337.
(67) Eisenwiener, A.; Neuburger, M.; Kaden, T. A. *Dalton Trans.* **2007**, 218–233.
(68) Mernari, B.; Abraham, F.; Lagrenee, M.; Drillon, M.; Legoll, P. *J. Chem. Soc., Dalton Trans.* **1993**, 1707–1711.
(69) Konrad, M.; Wuthe, S.; Meyer, F.; Kaifer, E. *Eur. J. Inorg. Chem.* **2001**, 2233–2240.
(70) Ghedini, M.; Neve, F. *Polyhedron* **1985**, *4*, 497–503.
(71) Noël, G.; Röder, J. C.; Dechert, S.; Pritzkow, H.; Bolk, L.; Mecking, S.; Meyer, F. *Adv. Synth. Catal.* **2006**, *348*, 887–897.
(72) Röder, J. C.; Meyer, F.; Pritzkow, H. *Chem. Commun.* **2001**, 2176–2177.

Scheme 2.[a]

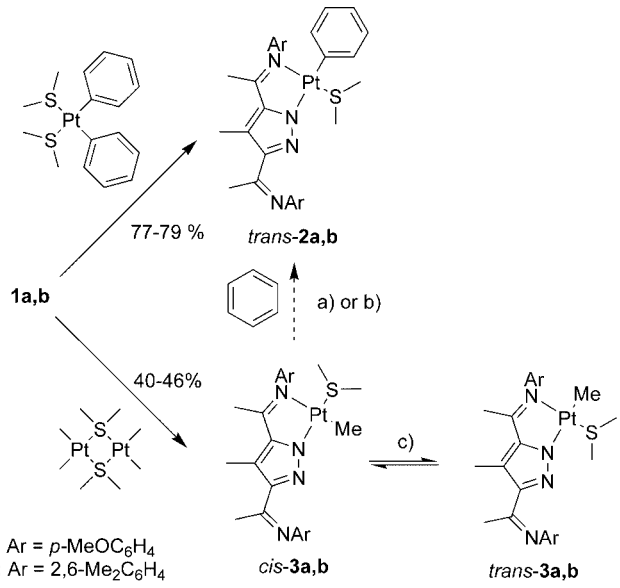

[a] Reaction conditions: a) Ar = 4-methoxyphenyl, 60 h 110 °C, conversion >50% (ESI-MS and ^{1}H NMR); b) Ar = 2,6-dimethylphenyl, 2 days, 130 °C, traces of **2b** observed by ESI-MS; c) DCM, RT, 10 days.

mononuclear complexes. As activation of the N−H bond of the related 2-(*N*-arylimino)pyrroles by $[(Me_2S)PtMe_2]_2$ is documented,[21] we investigated the reactivity of **1a**,**b** with $[(Me_2S)PtMe_2]_2$ and $(Me_2S)_2PtPh_2$ (Scheme 2).

The reaction of **1a**,**b** with $(Me_2S)_2PtPh_2$ afforded the mononuclear platinum(II) phenyl complexes *trans*-**2a**,**b** in good yields (the *cis* and *trans* notation are attributed according to the relative position of the pyrazolate nitrogen and the aryl or alkyl ligand). Remarkably, only one of the two possible isomers was formed, which shows that the pyrazolate and imine nitrogen atoms are electronically different.

Complexes *trans*-**2a**,**b** were characterized crystallographically (see Figure 1). In both compounds, the platinum center adopts the expected square-planar geometry, which is slightly distorted due to the acute (∼77°) bite angle of the ligand. The free sides of the ligands exhibit a N−C−C−N torsion angle of about 180°, which allows conjugation of the imine group with the pyrazolate ring but avoids the methyl−methyl repulsion that would arise at a 0° angle. The main geometrical difference between *trans*-**2a** and *trans*-**2b** is the orientation of the coordinated SMe_2 molecule, of which the two methyl groups are located on the same side of the coordination plane in **2a** but not so in **2b**. This discrepancy is likely due mainly to crystal packing forces. In both cases only one S-Me ^{1}H NMR signal is observed in solution, indicating a low rotational barrier around the Pt−S bond.

The ligands **1a**,**b** reacted with $[(Me_2S)PtMe_2]_2$ to yield mainly the *cis* isomer of the mononuclear complexes **3a**,**b**, which were isolated in moderate yield (see Scheme 2) and were fully characterized. Upon storage of *cis*-**3a**,**b** in CD_2Cl_2 solution at room temperature, new peaks appeared in the ^{1}H NMR spectra (see Figure 2), which were assigned to *trans*-**3a**,**b**.

The stereochemical assignment of **3a**,**b** was made mainly on the basis of ^{1}H NMR data as described here for **3a** (see Figure 2). Going from *cis*-**3a** to *trans*-**3a**, the SMe_2 signal is shifted downfield by 0.62 ppm, while the Pt-Me signal is shifted upfield by 1.09 ppm, which we attribute to the shielding effect of the *p*-methoxyphenyl moiety on the SMe_2 and Pt-Me protons of

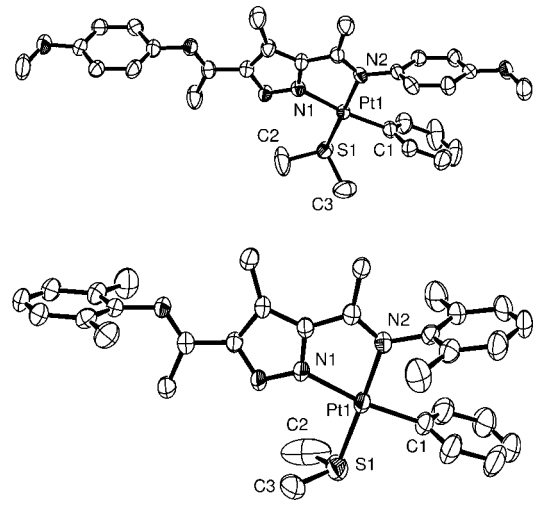

Figure 1. ORTEP representations of the X-ray crystal structures of *trans*-**2a** (top) and *trans*-**2b** (bottom). Ellipsoids are drawn at 50% probability. Selected distances [Å], angles [deg], and torsion angles [deg]: *trans*-**2a**: Pt1−C1 2.011, Pt1−S1 2.259, Pt1−N1 2.068, Pt1−N2 2.052, C1−Pt1−N1 172.0, S1−Pt1−N2 178.5, C1−Pt1−S2 85.6, C1−Pt1−N2 94.7, N1−Pt1−N2 77.4, N1−Pt1−S1 102.2, N1−Pt1−S1-C2 26.4, N1−Pt1−S1-C3 133.8. *trans*-**2b**: Pt1−C1 2.028, Pt1−S1 2.266, Pt1−N1 2.079, Pt1−N2 2.063, C1−Pt1−N1 171.5, S1−Pt1−N2 175.5, C1−Pt1−S1 87.6, C1−Pt1−N2 94.8, N1−Pt1−N2 77.8, N1−Pt1−S1 100.0, N1−Pt1−S1−C2 42.7, N1−Pt1−S1−C3 59.0.1.

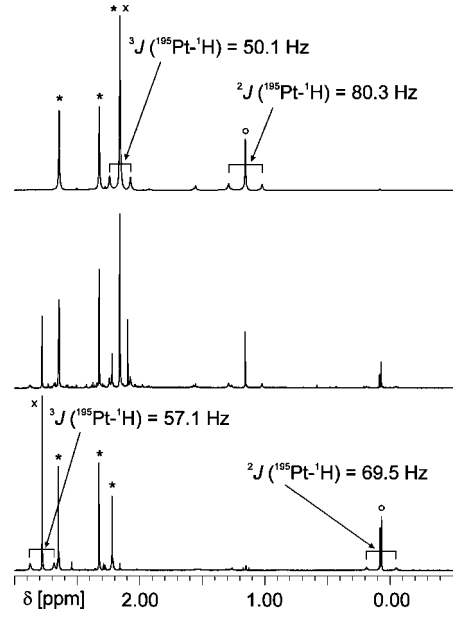

Figure 2. δ 0−3 ppm region of the ^{1}H NMR spectra of *cis*-**3a** (top), *trans*-**3a** (bottom), and a solution of *cis*-**3a** equilibrated for 10 days at room temperature. Peaks assigned to the bmimp ligand, coordinated Me_2S, and Pt-Me are marked with *, ×, and °, respectively.

the *cis* and *trans* isomers, respectively. Furthermore, for the related [2-(*N*-arylimino)pyrrolide]PtMe(SMe_2) complexes, Iverson et al.[21] reported $^3J(^{195}Pt-^1H)$ of 51 vs 58 Hz for Pt-SMe_2 and $^2J(^{195}Pt-^1H)$ of 79−80 vs 73 Hz for Pt-Me coupling constants of the *cis* and *trans* isomers, respectively. We find very similar values for *cis*- and *trans*-**3a**, which support our stereochemical assignment.

In order to confirm this assignment, we looked for conditions that would allow the isolation of *trans*-**3a**. We found that upon

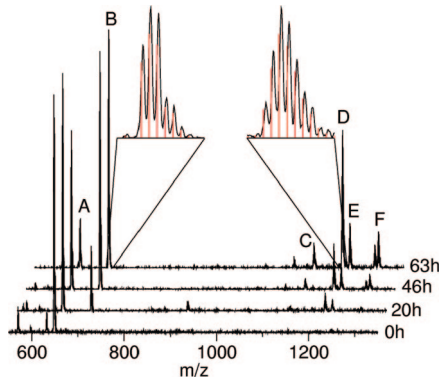

Figure 3. Time evolution of the mass spectra obtained from samples of a ca. 7 mM solution of *cis*-**3a** in benzene heated at 110 °C, and observed (black) and calculated (red) isotope patterns for peaks B and D. Peak assignment: A: $[\mathbf{3a} + H]^+$, B: $[\mathbf{2a} + H]^+$, C: $[(bmimp)_2Pt_2CH_3]^+$, D: $[(bmimp)_2Pt_2C_6H_5]^+$, E: $\{[(bmimp)_2Pt_2(CH_3)(C_6H_5)]^+ + H\}$ F: $\{[(bmimp)_2Pt_2(C_6H_5)]^+ + H\}$.

reaction of **1a** and $[(Me_2S)PtMe_2]_2$ in toluene, *cis*-**3a** precipitates, leaving mainly *trans*-**3a** in the liquid phase, from which it was isolated in 8% yield and fully characterized. Equilibration at room temperature over 10 days starting from either pure *cis*- or pure *trans*-**3a** yielded a *cis*/*trans* mixture in an approximate 3:1 ratio. An equilibrium ratio of about 2:1 was observed for *cis*-**3b** to *trans*-**3b**.

In order to test their ability to activate aromatic C−H bonds, **3a** and **3b** were heated in benzene, and the reaction was monitored by recording ESI-MS spectra of samples diluted in dichloromethane. As seen in Figure 3, when a solution of **3a** in benzene is heated at 110 °C in a closed vessel, the peak of protonated **3a** (*m*/*z* 648), gradually disappears, while the peak of protonated **2a** (*m*/*z* 710) grows, showing that the C−H activation reaction $\mathbf{3a} + C_6H_6 \rightarrow \mathbf{2a} + CH_4$ is taking place. Simultaneously, other peaks appear at higher masses, corresponding to dimeric species presumably formed by the substitution of SMe_2 in **2a** or **3a** by one of the free nitrogens of a second molecule. In order to check the identity of the main product, the mixture was evaporated to dryness after 60 h reaction time, and a ^{1}H NMR spectrum of the residue in CD_2Cl_2 was recorded (see Supporting Information). The main peaks correspond to those of independently synthesized *trans*-**2a**.

When a solution of **3b** was heated to 130 °C for several days, only traces of the C−H activation product could be observed by ESI-MS, together with dimeric species. As the *cis*−*trans* equilibration takes place already at room temperature for both **3a** and **3b**, it is expected to be fast at 110−130 °C. Thus, the actual C−H activation step could proceed from either isomer. Therefore, the lower reactivity of **3b** as compared to **3a** cannot be explained by slow isomerization, but likely stems from the increased steric bulk around the Pt(II) center that slows down the presumably associative exchange of SMe_2 for benzene, which is likely to be the rate-determining step in this reaction.[34]

The ability of the free binding site of *cis*-**2a**,**b** and *trans*-**3a**,**b** to accept a metal ion was tested by reacting these compounds with copper(I) chloride (Scheme 3), affording deep red colored solutions of the mixed complexes **4a**,**b** and **5a**,**b**.

The positive ion ESI-MS spectra of these solutions all feature the 2:1 complex cations of **4a**,**b** and **5a**,**b**, respectively, as the most intense signal, and both the isotope pattern and the fragmentation products are consistent with this assignment. In most cases, a weak signal corresponding to the incorporation of an extra CuCl unit in the cation is observed, but this ion is likely to be formed during the electrospray process. Furthermore, the $[CuCl_2]^-$ anion is observed for all four compounds, sometimes accompanied by a low signal corresponding to $[Cu_2Cl_3]^-$.

The ^{1}H and ^{13}C NMR spectra of **4a** and **5a** exhibit sharp signals corresponding to a single species, which were assigned to the ionic structure depicted in Scheme 3.

In order to confirm this assignment, we grew crystals of **4a** suitable for X-ray crystallography from a benzene solution. The crystal structure of **4a** (Figure 4) contains two independent but similar C_2 symmetrical cations. The copper(I) center has a distorted tetrahedral coordination sphere, the planes of the two ligands making an angle of approximately 90°. The length difference of ∼0.05 Å between the Cu−N3 and Cu−N4 bonds shows that the pyrazolate bridge is a slightly better σ-donor than the *N*-arylimine. The opposite trend seen in Pt−N bonds for both *trans*-**2a**,**b** and **4a**,**b** is likely due to the strong *trans* influence of the phenyl ligand that weakens, and thus lengthens, the pyrazolate N−Pt bond. In both independent cations, the Me_2S ligand is oriented in such a way that the remaining lone pair on the sulfur atom would point toward the Cu(I) center. However, the S−Cu distance of more than 3.6 Å is too large for chemical binding, and thus the orientation of the Me_2S ligands is most probably driven by the minimization of steric repulsion. Besides this orientation change of the Me_2S ligand, the geometry around the Pt(II) centers is rather unaffected by coordination to copper(I). The Pt−Cu distance of about 4.4 Å is too large for metal−metal binding, but could in principle allow cooperative behavior.[61]

Very broad signals were observed in the room-temperature ^{1}H NMR spectra of **4b** and **5b**, suggesting chemical exchange, and therefore the temperature dependence was studied. The methyl regions of ^{1}H NMR spectra of **4b** at temperatures ranging from −40 °C to room temperature are presented in Figure 5. When cooling the sample, the sharp signal assigned to the pyrazolate-bound methyl group at δ 2.58 ppm broadens and finally splits into two signals in an approximate 3:4 ratio, indicating the presence of two interchanging species. The most common structures for CuCl adducts of diimine (NN) ligands, depicted in Scheme 3, are the ionic, four-coordinate complex $[(NN)_2Cu][CuCl_2]$[73−76] (**4b**), the monomeric, T-shaped three-coordinate complex (NN)CuCl[76,77] (**6b**), and the corresponding dimer (NN)Cu(μ-Cl_2)Cu(NN)[76] (**6b′**). Structures **6b** and **6b′** possess a symmetry plane perpendicular to the plane of the 2,6-dimethylphenyl unit, while **4b** does not. Thus, for structure **4b**, the two S-Me groups as well as the two *ortho*-methyl groups of the ligand phenyl ring are magnetically different if the corresponding rotations are hindered, which would yield nine different signals of equal intensities. On the other hand, species **6b** or **6b′**, in which the two sides of the ligand are symmetry equivalent, should yield three signals with a relative intensity of 1 (the three methyl groups of the central unit) and three signals with an intensity of 2 (both 2,6-dimethylphenyl units and the SMe_2 ligand), a total of six signals. At −40 °C, 13 peaks are resolved in the methyl region. Band width and overlap

(73) Skelton, B. W.; Waters, A. F.; White, A. H. *Aust. J. Chem.* **1991**, *44*, 1207–1215.
(74) Mirkhani, V.; Harkema, S.; Kia, R. *Acta Crystallogr.* **2004**, *C60*, m343−m344.
(75) Yu, J.-H.; Lü, Z.-L.; Xu, J.-Q.; Bie, H-Y.; Lu, J.; Zhang, X. *New J. Chem.* **2004**, *28*, 940–945.
(76) Dieck, H. T.; Stamp, L. *Z. Naturforsch.* **1990**, *45b*, 1396–1382.
(77) Healy, P. C.; Pakawatchai, C.; White, A. H. *J. Chem. Soc., Dalton Trans.* **1985**, 2531–2539.

Scheme 3.[a,b]

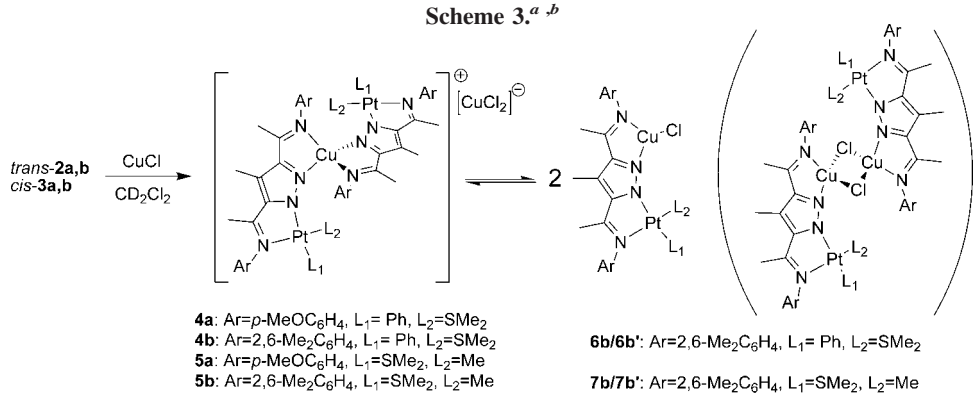

[a] The rightmost equilibrium was observed only for Ar = 2,6-$Me_2C_6H_4$. [b] The dimeric structure in parentheses was ruled out by the concentration independence of the ratio between the equilibrating species (see text).

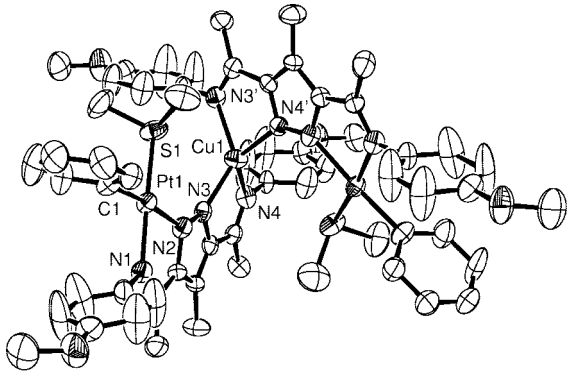

Figure 4. ORTEP plot of one of the two crystallographically independent cations in the crystal cell of **4a**. Ellipsoids are drawn at 50% probability. Selected distances [Å], angles [deg], and torsion angles [deg] (values for the second cation given in parentheses): Pt1−C1 2.025 (2.033), Pt1−S1 2.262 (2.262), Pt1−N1 2.055 (2.048), Pt1−N2 2.072 (2.094), Pt1−Cu1 4.409 (4.382), Pt1−Pt1′ 6.321 (6.135), Cu1−N3 2.019 (1.998), Cu1−N4 2.065 (2.047), N2−N3 1.334 (1.341), Cu1−S1 3.670 (3.649), C1−Pt1−S1 91.2 (92.6), C1−Pt1−N1 95.7 (93.5), N1−Pt1−N2 78.2 (77.6), S1−Pt1−N2 94.9 (97.0), C1−Pt1−N2 173.9 (170.0), S1−Pt−N1 172.6 (173.4), N3−Cu1−N4 79.3 (80.5), N3−Cu−N3′ 125.4 (126.2), N3−Cu1−N4′ 130.2 (128.4), N4−Cu1−N4′ 119.9 (119.4), Pt1−Cu1−Pt1′ 91.6 (88.9), Pt1−N2−N3−Cu1 30.9 (19.8).

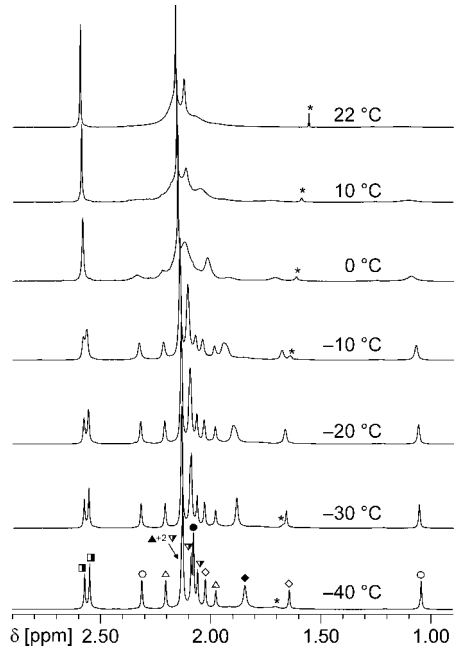

Figure 5. Plot of the methyl region of the ^{1}H NMR spectra of **4b** ⇄ **6b** in solution recorded at different temperatures. Peak assignments based on the EXSY spectrum (see Supporting Information): pyrazolate-*Me*, □; 2,6-*Me*$_2$Ph-N(Cu), ○; 2,6-*Me*$_2$Ph-N(Pt), Δ; N=C*Me*, ▽; S*Me*$_2$, ◇. Open symbols label peaks assigned to **4b**, filled symbols label peaks assigned to **6b**, and half-filled symbols label peaks that could belong to either **4b** or **6b**. The residual water signal is marked with *.

preclude an accurate integration of many peaks, but one can count 10 peaks with an intensity corresponding to one methyl group, two peaks (δ 2.08 and 1.84 ppm) corresponding to two methyl groups, and one peak (δ 2.13 ppm) corresponding to four methyl groups. Assuming some peak overlap, the observed spectrum is consistent with the presence of one symmetrical and one unsymmetrical species in equilibrium. This was confirmed by an EXSY spectrum recorded at −25 °C, which allowed us to partially assign the resonances as shown in Figure 5 (see Supporting Information for details). Thus, consistently with the ESI-MS data, we propose that one of the structures is the unsymmetrical **4b**. In order to distinguish between **6b** and **6b′**, we recorded ^{1}H NMR spectra of ca. 20, 40, and 60 mM solutions at −40 °C and observed no concentration dependence of the ratio between the two species. Consequently, there must be the same number of species on both sides of the equilibrium depicted in Scheme 3, and the second structure must be **6b**. The existence of a second species is likely due to the steric bulk introduced by the *ortho*-methyl groups of the ligand phenyl ring, which destabilizes the 2:1 complex cation of **4b**.

The ^{1}H NMR spectrum of a ca. 88 mM solution of **5b** in CD_2Cl_2 at −40 °C exhibits mainly 10 peaks with approximately equal intensities in the methyl region (see Figure 6). The peak at δ 0.83 ppm has ^{195}Pt satellites with $^2J(^{195}\text{Pt}-^1\text{H})$ = 75 Hz and is assigned to the Pt-*Me* group. The number of peaks and their relative intensities suggest that the unsymmetrical ionic structure **5b** is the main species in solution. However, the small peak at δ 1.49 ppm with $^2J(^{195}\text{Pt}-^1\text{H})$ = 76 Hz indicates the presence of a second species in an approximate 1:6 equilibrium ratio. Not all the peaks arising from this second species could be observed, as some are most probably hidden under the peaks of **5b**, but we tentatively assign it to a monomeric (**7b**) or dimeric (**7b′**) symmetrical structure. The equilibrium ratio was found to shift from ca. 1:6 to ca. 1:4 when the concentration was taken down from 88 mM to 22 mM. If the second species were dimeric (**7b′**), the ratio should decrease rather than increase at lower concentration, and thus the latter hypothesis can be ruled out. The observed equilibrium shift is too small to be due to a monomer−dimer equilibrium, but could be explained by

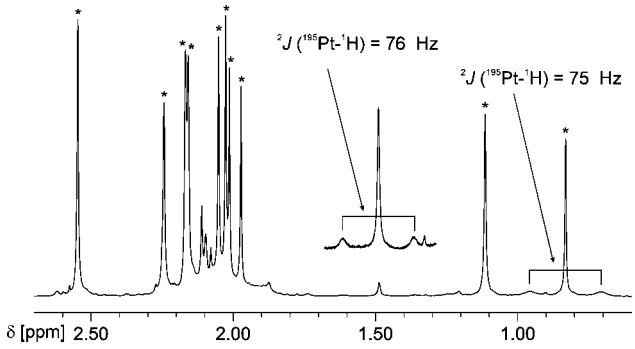

Figure 6. Plot of the methyl region of the ^{1}H NMR spectra of **5b** ⇄ **7b** in solution recorded at −40 °C. The peaks assigned to **5b** are marked with *.

some extent of ion pairing of **5b** at high concentration. One could argue that with a 1:6 equilibrium ratio, the **5b** ⇄ **7b** exchange should cause only a slight broadening of the peaks of the most abundant species **5b**. However, one has to consider that the magnetically nonequivalent 2- and 6- methyl groups do exchange via the sequence **5b** → **7b** → **5b**, as the 2- and 6-positions are equivalent in the symmetrical species **7b**. This exchange causes the extensive broadening observed at higher temperatures.

Steric Repulsion Based Strategy. C−H activation by the mononuclear complexes **3a**,**b** has been found to be slow even at high temperatures, which is likely due to strong binding of the dimethylsulfide ligand that slows down its exchange for benzene in the first coordination sphere of platinum. One way to generate similar species with a weaker protecting ligand is the *in situ* protolysis of dialkyl or diaryl species with a weakly coordinating acid. Thus, we prepared and characterized mononuclear platinum(II) diphenyl complexes of the 3,5-bis(iminoacetyl)pyrazole ligands, anticipating that the bulk of the phenyl ligands would hamper the formation of dinuclear species.

Deprotonation of **1a**,**b** with KO^{t}Bu followed by reaction with $(Me_2S)_2PtPh_2$ afforded the mononuclear anionic complexes **8a**,**b** in good yields (see Scheme 4). Both complexes were fully characterized, and **8b** was studied by X-ray diffraction (Figure 7).

In the crystal structure of **8b**, the ligands coordinated to platinum(II) adopt the expected distorted square-planar geometry. The Pt−C bond lengths (2.005 and 2.004 Å) are almost identical and are significantly shorter than in the monophenyl complex **2b** (2.025 Å), while the *imine*-N−Pt bond is longer by 0.068 Å, which we attribute to the larger *trans* influence of a phenyl ligand as compared to Me_2S. The potassium ion is chelated by two nitrogen atoms of the ligand in a highly unsymmetrical way, with K−N distances of 2.741 and 2.955 Å for the pyrazolate and imine nitrogens, respectively, and with an acute bite angle of 57°. The coordination sphere of the potassium ion is completed by one phenyl ligand from the same molecule and two from the neighboring one, building an aromatic pocket around the ion.

With the mononuclear anionic complexes **8a**,**b** at hand, we investigated their ability to coordinate Cu(I) (Scheme 5). When a solution of 1 equiv of CuCl in acetonitrile is added to a solution of **8a**,**b** in the same solvent, a yellow precipitate forms, which contains KCl and the solvated Cu(I) complex **9a**,**b**. Extraction of this solid with benzene yielded orange solutions of the 2:2 complexes **10a**,**b**, which crystallized as red needles (**10a**) or orange plates (**10b**) upon vapor diffusion with hexane.

The accurate stoichiometry of the solvento complexes **9a**,**b** was not determined because the solid releases part of its acetonitrile content upon drying. However, crystallization of **9b** from warm acetonitrile allowed its characterization by X-ray diffractometry. The asymmetric unit of the crystal structure (Figure 8) consists of a monomeric heterobimetallic complex and two unbound acetonitrile molecules. The Cu(I) center is chelated by the free binding site of the bdmimp ligand, and its slightly distorted tetrahedral coordination sphere is completed by two η^1-bound acetonitrile molecules. The slightly distorted square-planar Pt(II) coordination is roughly identical to the one found in **8b**, except for a somewhat longer Pt1−N2 bond (2.106 vs 2.060 Å), which can be attributed to a decrease in the σ-donating ability of one of the pyrazolate nitrogen atoms arising when the second one is coordinated to copper. Further characterization of **9b** in solution was hampered by its ability to lose acetonitrile and convert to **10b** when dissolved in other solvents.

Vapor diffusion of hexane into solutions of **10a** and **10b** in benzene and dioxane, respectively, afforded crystals suitable for X-ray diffraction. The structure of **10a** (Figure 9) is tetranuclear with approximate C_2 symmetry, in which both copper atoms lie on the quasi-C_2 axis with one platinum atom on each side, resulting in an almost planar arrangement of the four metals. The Cu−Cu distance is 2.753 Å, which is typical for a cuprophilic interaction.[78] The Cu2 center is chelated by two nitrogen atoms of each bmimp ligand, forming a highly distorted tetrahedral coordination environment, in which the N3−Cu2−N3′ angle opens up to 150.7° to allow for the close Cu−Cu contact. The large difference in Cu−N3 and Cu−N4 bond lengths (∼1.97 vs ∼2.21 Å) is noteworthy, indicating that the pyrazolate nitrogens are more tightly bound than the imine nitrogens. The most peculiar feature of **10a**, though, is the coordination environment of the Cu1 center. In addition to the aforementioned Cu−Cu interaction, it consists of two close contacts with the Pt(II) centers (2.66 and 2.74 Å), supported by a coordination to the *ipso* carbons of two platinum-bound phenyl ligands. One of the *ortho* carbons of these phenyl groups is at a shorter distance from the Cu1 center than the other (2.51 and 2.41 vs 2.82 and 3.06 Å). This orientation could indicate a distorted η^2-coordination, but may also be due mainly to steric repulsion, as it places the phenyl rings parallel to the neighboring bmimp ligand plane. Therefore, the much shorter C^{ipso}−Cu distances (2.07 and 2.14 Å) entice us to describe this interaction mainly as η^1-phenyl coordination.

The structure of **10b** (Figure 10) shows a planar tetrametallic arrangement similar to that for **10a**. The main difference is the rotation of the arm of one of the bdmimp ligands by 180°, breaking one imine-N−Cu bond. This discrepancy is most likely due to the increased steric bulk of the 2,6-dimethylphenyl moiety as compared to that of 4-methoxyphenyl, which prevents the two imine nitrogens from being coordinated at the same time to the Cu2 atom. As a result, the Cu2 center adopts a distorted planar, T-shaped coordination. The remaining Cu2−N4 bond is strikingly longer than in **10a** (2.44 vs 2.21 Å) and, thus, is expected to be relatively weak. The coordination around Cu1 is hardly affected by this change in the Cu2 environment, the main difference being a slight shortening of the Pt−Cu contacts from 2.74 and 2.66 Å in **10a** to 2.57 and 2.57 Å in **10b**.

The preparation of compounds with Pt(II)−Cu(I) contacts supported by two $R_2PCH_2PR_2$ (R = phenyl,[79] cyclohexyl[80]) ligands and of Cu(I) complexes of a metallamacrocycle incorporating two Pt(II)Me_2 units[81] has been documented, but to our knowledge, **10a** and **10b** are the first structurally characterized compounds that exhibit a dative Pt→Cu bond without a bridging

(78) Hermann, H. L.; Boche, G.; Schwerdtfeger, P. *Chem.−Eur. J.* **2001**, *7*, 5333–5342.

Scheme 4

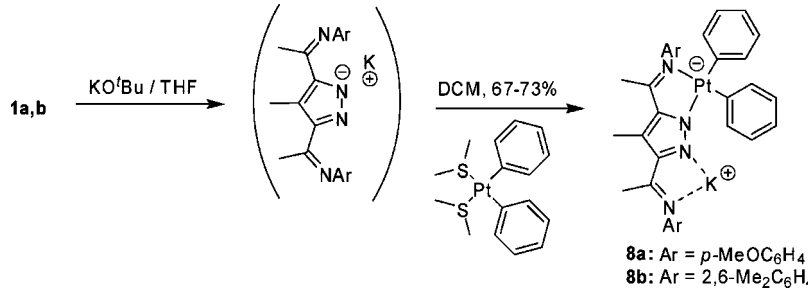

Scheme 5.[a]

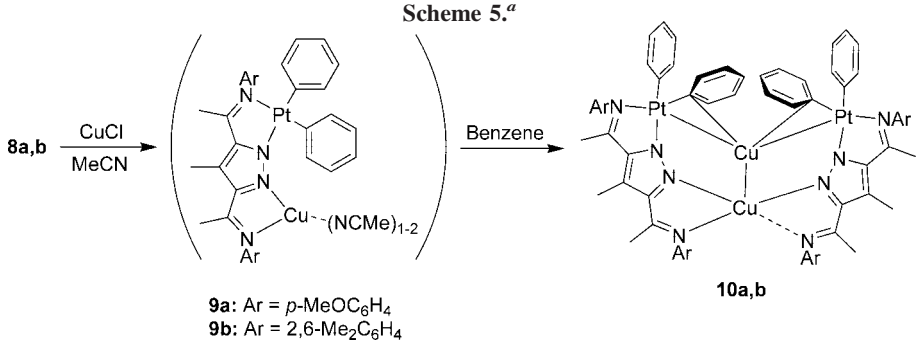

[a] The coordination represented by a dashed line is observed only for **10a**.

ligand. The Pt(II)−Cu(I) binding in **10a**,**b** is structurally related to the dative Pt→Ag bond observed in several compounds incorporating hard σ-donor ligands on platinum,[82−87] where the electron-rich Pt(II) center acts as a Lewis base.

The behavior of **10a**,**b** in solution was investigated by means of ^{1}H NMR. At room temperature, the ^{1}H NMR spectrum of

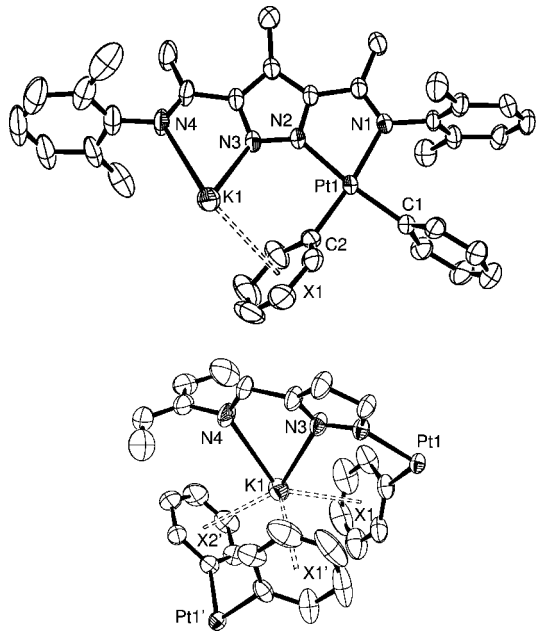

Figure 7. ORTEP plot of the X-ray crystal structure of **8b**. Ellipsoids drawn at 50% probability. Top: view of the asymmetric cell. Bottom: view of the atoms within 5 Å of K1. The centroids of aromatic rings are labeled X. Selected distances [Å], angles [deg], and torsion angles [deg]: Pt1−C1 2.005, Pt1−C2 2.004, Pt1−N1 2.123, Pt1−N2 2.060, Pt1−K1 4.390, N2−N3 1.321, K1−N3 2.741, K1−N4 2.955, K1-X1 3.056, K1−X1′ 3.350, K1−X2 3.111, C1−Pt1−N1 96.9, N1−Pt1−N2 76.8, N2−Pt1−C2 96.8, C1−Pt1−C2 89.6, N1−Pt1−C2 172.9, N2−Pt1−C1 173.6, N1−K1−N4 57.3, Pt1−N2−N3−K1 33.7.

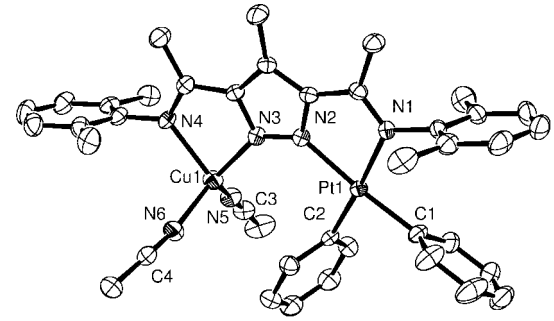

Figure 8. ORTEP representation of the X-ray crystal structure of **9b**. Ellipsoids drawn at 50% probability. For clarity, two unbound molecules of acetonitrile present in the asymmetric unit are omitted. Selected distances [Å], angles [deg], and torsion angles [deg]: Pt1−C1 2.022, Pt1−C2 1.990, Pt1−N1 2.111, Pt1−N2 2.106, Pt1−Cu1 4.369, Cu1−N3 2.042, Cu1−N4 2.143, Cu1−N5 1.999, Cu1−N6 1.952, N2−N3 1.325, C1−Pt1−C2 88.1,C1−Pt1−N1 96.2, N1−Pt1−N2 76.6, C2−Pt2−N2 99.2, C1−Pt1−N2 172.3, C2−Pt1−N1 175.7, N3−Cu1−N4 78.8, N3−Cu1−N5 120.3, N3−Cu1−N6 119.4, N4−Cu1−N5 119.9, N4−Cu1−N6 99.6, N5−Cu1−N6 112.5, Cu1−N5−C3 170.7, Cu1−N6−C4 172.2, Pt1−N2−N3−Cu1 1.1.

10a exhibits two sharp lines at 3.78 and 3.68 ppm, corresponding to the Ar-O*Me* protons, but only two broad peaks between 2 and 2.7 ppm, where one would expect three for an unsymetrically coordinated bmimp ligand. In order to elucidate whether this behavior would be due to some chemical exchange process, we recorded spectra at temperatures ranging from −30 °C up to room temperature (Figure 11). The spectra clearly show that there are two different species present, for which the interconversion rate is fast compared to the ^{1}H NMR time scale at room temperature and slow at −30 °C. The ratio between the two species is temperature dependent, which rules out the possibility that all the signals belong to a single species containing two different ligands. Our first hypothesis on the nature of the two species was that there would be an equilibrium between a monomeric form and the dimer observed in the crystal structure. If this were the case, then the ratio between the two species

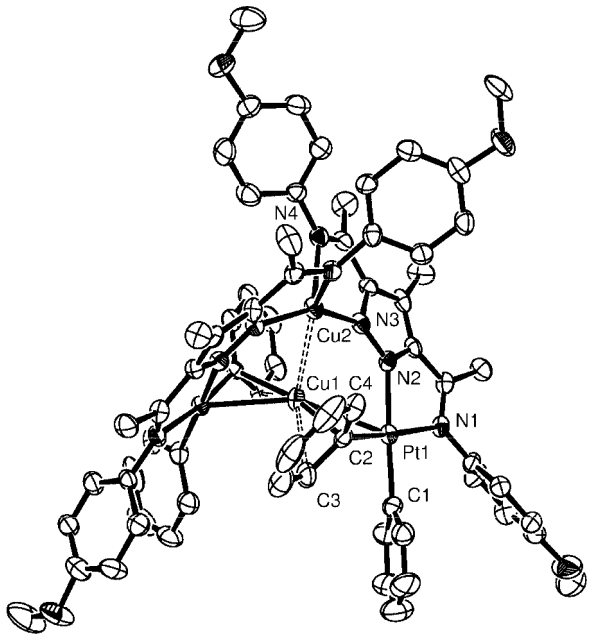

Figure 9. ORTEP representation of the X-ray crystal structure of **10a**. Ellipsoids drawn at 50% probability. Selected distances [Å], angles [deg], and torsion angles [deg] (values for the approximate C_2 symmetry equivalents given in parentheses): Pt1−C1 1.990 (1.992), Pt1−C2 2.024 (2.015), Pt1−N1 2.117 (2.128), Pt1−N2 2.064 (2.058), Pt1−Cu1 2.744 (2.658), C2−Cu1 2.069 (2.145), C3−Cu1 2.514 (2.409), C4−Cu1 2.824 (3.056), Cu1−Cu2 2.753, Cu2−N3 1.983 (1.963), Cu2−N4 2.206 (2.206), N2−N3 1.342 (1.346), C1−Pt1−C2 87.0 (88.6), C1−Pt1−N1 96.0 (96.1), N1−Pt1−N2 77.3 (76.3), C2−Pt1−N2 100.1 (99.2), C1−Pt1−N2 172.4 (172.1), C2−Pt1−N1 172.5 (172.5), Pt1−C2−Cu1 84.2 (79.4), Pt1−Cu1−Pt1′ 155.2, Pt1−Cu1−Cu2 101.8 (99.0), C2−Cu1−C2′ 165.6, C2−Pt1−Cu1 48.6 (52.5), N3−Cu2−N4 79.1 (78.2), N3−Cu2−N3′ 150.7, N4−Cu2−N4′ 89.1, N2−Pt1−C2−C3 138.7 (142.4), Pt1−Cu2−Cu1−Pt1′ 166.6, Pt1−N2−N3−Cu2 17.5 (−12.9).

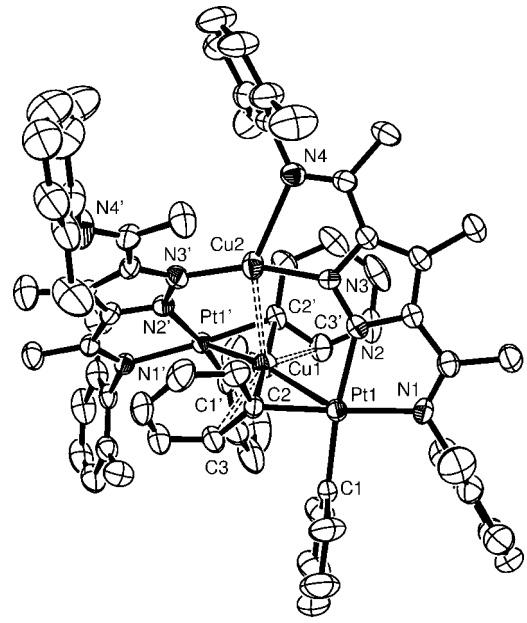

Figure 10. ORTEP representation of the X-ray crystal structure of **10b**. Ellipsoids drawn at 50% probability. For clarity, 1.5 molecules of 1,4-dioxane present in the asymmetric unit are omitted. Selected distances [Å], angles [deg], and torsion angles [deg]: Pt1−C1 2.013, Pt1′−C1′ 2.004, Pt1−C2 2.042, Pt1′−C2′ 2.031, Pt1−N1 2.106, Pt1′−N1′ 2.094, Pt1−N2 2.095, Pt1′−N2′ 2.122, Pt1−Cu1 2.570, Pt1′−Cu1 2.574, C2−Cu1 2.110, C2′−Cu1 2.144, C3−Cu1 2.530, C3′−Cu1 2.476, Cu1−Cu2 2.760, Cu2−N3 1.944, Cu2−N3′ 1.937, Cu2−N4 2.444, C1−Pt1−C2 87.6, C1′−Pt1′−C2′ 86.7, C1−Pt1−N1 96.0, C1′−Pt1′−N1′ 94.6, N1−Pt1−N2 76.6, N1′−Pt1′−N2′ 77.5, C2−Pt1−N2 100.1, C2′−Pt2′−N2′ 101.2, C1−Pt1−N2 172.2, C1′−Pt1′−N2′ 172.1, N1−Pt1−C2 169.8, N1′−Pt1′−C2′ 176.0, Pt1−C2−Cu1 76.5, Pt1′−C2′−Cu1 76.1, Pt1−Cu1−Pt1′ 165.1, Pt1−Cu1−Cu2 100.1, Pt1′−Cu1−Cu2 94.6, C2−Cu1−C2′ 144.0, C2−Pt1−Cu1 53.0, C2′−Pt1′−Cu1 53.9, N3−Cu2−N4 74.9, N3−Cu2−N3′ 161.6, N3′−Cu2−N4 123.2, N2−Pt1−C2−C3 146.8, N2′−Pt1′−C2′−C3′ 139.5, Pt1−Cu2−Cu1−Pt1′ 177.1, Pt1−N2−N3−Cu2 7.4, Pt1′−N2′−N3′−Cu2 3.0.

should be dependent on the overall concentration of the sample. However, this ratio was found to be identical for 15, 30, and 45 mM solutions of **10a**. Consequently, we propose the following interpretation of our data, summarized in Figure 12: considering the fact that an "open" form is found in the crystal structure of **10b** (Figure 10), we postulate that a similar structure **A** also exists for **10a**. At room temperature, it rapidly interconverts with the "closed" structure **B**, yielding only one set of signals, some of which are broadened due to incomplete coalescence. This interconversion is frozen at −30 °C, while the intramolecular ligand exchange **A** ⇄ **A′** is still fast. This means that the free energy barrier for the fourth nitrogen atom coordination **A** ⇄ **B** is higher than the barrier for the exchange **A** ⇄ **A′**, implying that the latter has to be dissociative in nature.

The spectrum of **10b**, recorded at room temperature, exhibits seven peaks with comparable integrals in the methyl region, which indicates the presence of only one type of bdmimp ligand in which the two *ortho*-methyl groups on the imine aromatic ring are different. Thus, we can rule out the hypothesis of a rapid dissociation/recombination of the dimeric structure of **10b**, because it would involve the existence of a symmetrical intermediate in which the aforementioned methyl groups would be equivalent, affording two peaks with a relative integral of 2 and three with integral 1 instead of the actual seven equally intense peaks. The observation of only seven peaks shows that, although there are two different ligands in the crystal structure of **10b**, they must rapidly interconvert via a—presumably dissociative—ligand exchange at the Cu2 ion, depicted as the **A** ⇄ **A′** equilibrium in Figure 12. In order to test this interpretation, we recorded a spectrum at −70 °C, which exhibited an important broadening of several peaks. Even though no splitting of the peaks could be observed, this broadening supports the existence of the two species **A** and **A′**, whose interconversion becomes slow at low temperature. The fact that species **B** is not observed for **10b** is a result of the increased steric repulsion between the imine aromatic moieties of both bdmimp ligands, which would destabilize **B**.

The dynamic behavior exhibited in solution by the dimeric structures **10a**,**b** involving several coordination states around the copper atoms suggests that coordination and activation of small molecules should be possible. Furthermore, these dimers have the ability to break down to monomeric dinuclear complexes in the presence of coordinating ligands, as exemplified by the isolation of the acetonitrile adduct **9b**. Thus, they could possibly act as a reservoir for dinuclear complexes in a catalytic cycle.

Conclusions

Symmetrical, pyrazolate based bis-diimine ligands are easily accessible and can be used to prepare heteronuclear complexes in which each binding site is coordinated to a different metal. We applied two different strategies to prepare mononuclear

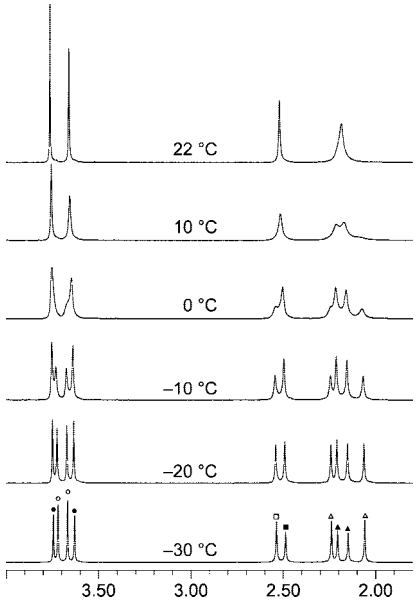

Figure 11. Methyl region of the ^{1}H NMR spectra of **10a** recorded at different temperatures in CD_2Cl_2. Peaks assigned to N=C*Me* groups are marked with triangles, pyrazolate-*Me* with squares, and *Me*O with circles. The two equilibrating species are distinguished by filled and open symbols.

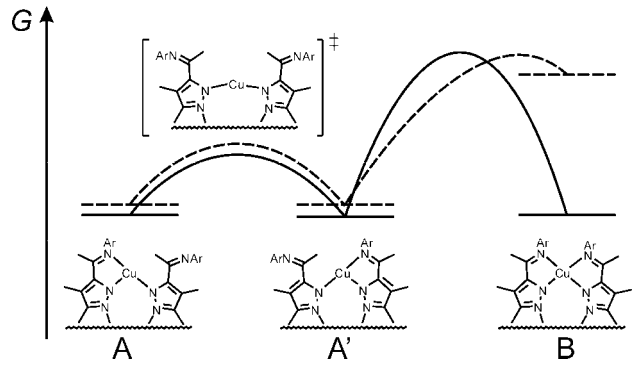

Figure 12. Proposed schematic potential energy surface for **10a** (solid) and **10b** (dashed) in solution.

complexes incorporating an organometallic platinum(II) moiety and their copper(I) adducts, using two electronically similar but sterically different ligands. First, we took advantage of the single acidic N−H bond in the protonated ligand, making it react with organometallic Pt(II) precursors in order to selectively prepare mononuclear Pt(II) complexes. One of these mononuclear complexes is active for the stoichiometric C−H activation of benzene, but only at high temperatures, while the more sterically hindered complex yielded only traces of the C−H activation product. These complexes can accommodate a Cu(I) center in their empty coordination site. Second, we made use of the sterical bulk of the $PtPh_2$ fragment to synthesize mononuclear anionic complexes as their potassium salt. Their complexation to copper(I) yielded neutral, dimeric structures built by several weak ligand−metal and metal−metal interactions, including dative Pt→Cu bonds. These dimers exhibit fluxional behavior in solution, and we expect them to easily break down to monomeric species in the presence of coordinating substrates, as demonstrated by the isolation of a solvated monomeric structure from acetonitrile. Throughout the study, we observed several differences in both structure and reactivity of the complexes induced by the different steric bulk of the two ligands we considered, which leads us to think that this factor could be critical for future catalytic application. The reactivity and possible catalytic activity of the described complexes is the subject of further investigation in our laboratories.

Experimental Part

General Procedures. Solvents were obtained commercially in p.a. quality and used as received. For reactions involving metal complexes, solvents were distilled under nitrogen over sodium (hexane, toluene), Na/K alloy (diethylether), potassium (tetrahydrofuran), or CaH_2 (acetonitrile, dichloromethane). All chemical manipulations involving metal complexes were performed in an inert atmosphere using standard Schlenk and glovebox techniques unless otherwise stated. ^{1}H and ^{13}C NMR spectra were recorded on Varian Gemini 300 and Varian Mercury 300 instruments. ^{1}H and ^{13}C chemical shifts are reported in ppm relative to tetramethylsilane, using residual solvent proton and ^{13}C resonances as internal references. Multiplicities are indicated as s (singlet), d (doublet), t (triplet), and dd (doublet doublet), while apparent singlets, doublets, and triplets are indicated by "s", "d", and "t", respectively. For peak assignment, benzenic rings are abbreviated Ar and pyrazole rings Pz. Elemental analyses were carried out by the Mikrolabor of the Laboratorium für Organische Chemie of ETH Zürich. Melting points are uncorrected and were measured in unsealed capillaries. Organolithium reagents were titrated using the procedure of Watson and Eastham.[88] 3,5-Diacetyl-4-methylpyrazole[89,90] and $Pt_2(CH_3)_4(\mu\text{-}Me_2S)_2$[91] were prepared according to literature procedures. *cis*-$PtPh_2(SMe_2)_2$ was prepared using a modification of a literature procedure.[92] All other chemicals were obtained commercially and used as received.

Ligand Syntheses. 3,5-Bis(4-methoxyphenyliminoacetyl)-4-methylpyrazole (bmimpH, 1a). A mixture of 3,5-diacetyl-4-methylpyrazole (700 mg, 5 mmol), *p*-methoxyaniline (2.5 g, 20 mmol), and formic acid (50 mg, 1 mmol) in methanol (10 mL) was stirred for 15 h at room temperature. Filtration, washing with methanol (4 × 5 mL) and diethyl ether (5 mL), and drying *in vacuo* yielded the product as an off-white powder (1.44 g, 77%). Mp: ≥ 219 °C (dec). ^{1}H NMR (DMSO-d_6, 300 MHz): δ 13.46 (br, 1H, N*H*), 6.94 (d, ^3J(H−H) = 8.7 Hz, 4H, Ar$H^{2,6}$), 6.77 (d, ^3J(H−H) = 8.6 Hz, 4H, Ar$H^{3,5}$), 3.75 (s, 3H, OCH_3), 2.57 (s, 3H, Pz-CH_3), 2.22 (s, 6H, ArN=C(CH_3)-Pz). No ^{13}C NMR spectrum could be recorded due to poor solubility in common solvents. ESI-MS (DCM), positive ion scan: *m/z* 377 ([M + H]$^+$). Anal. Calcd for $C_{18}H_{20}N_4O$: C 70.11, H 6.54, N 18.17. Found: C 69.85, H 6.63, N 18.24.

3,5-Bis(2,6-dimethylphenyliminoacetyl)-4-methylpyrazole (bdmimpH, 1b). A solution of 3,5-diacetyl-4-methylpyrazole (434 mg, 2.6 mmol), 2,6-dimethylaniline (1.9 g, 15.7 mmol), and *p*-toluenesulfonic acid monohydrate (50 mg, 0.26 mmol) in toluene (30 mL) was refluxed for 64 h using a Dean−Stark water separator. The solvent was then evaporated under reduced pressure, and the residue was washed with methanol (10 mL + 3 × 4 mL) and dried

(79) Cooper, G. R.; Hutton, A. T.; Langrick, C. R.; McEwan, D. M.; Pringle, P. G.; Shaw, B. L. *J. Chem. Soc., Dalton Trans.* **1984**, 855–862.
(80) Xia, B.-H.; Zhang, H.-X.; Che, C.-M.; Leung, K.-H.; Phillips, D.-L.; Zhu, N.; Zhou, Z.-Y. *J. Am. Chem. Soc.* **2003**, *125*, 10362–10374.
(81) Song, H.-B.; Zhang, Z.-Z.; Hui, Z.; Che, C.-M.; Mak, T. C. W. *Inorg. Chem.* **2002**, *41*, 3146–3154.
(82) Arsenault, G. J.; Anderson, C. M.; Puddephatt, R. J. *Organometallics* **1988**, *7*, 2094–2097.
(83) Usón, R.; Forniés, J.; Tomás, M.; Ara, I.; Casas, J. M.; Martin, A. *J. Chem. Soc., Dalton Trans.* **1991**, 2253–2264.
(84) Forniés, J.; Navarro, R.; Tomás, M.; Urriolabeitia, E. P. *Organometallics* **1993**, *12*, 940–943.
(85) Forniés, J.; Ibáñez, S.; Martín, A.; Sanz, M.; Berenguer, J. R.; Lalinde, E.; Torroba, J. *Organometallics* **2006**, *25*, 4331–4340.
(86) Yamaguchi, T.; Yamazaki, F.; Ito, T. *J. Am. Chem. Soc.* **1999**, *121*, 7405–7406.
(87) Yamaguchi, T.; Yamazaki, F.; Ito, T. *J. Am. Chem. Soc.* **2001**, *123*, 743–744.

Table 1. Crystallographic Data for Compounds 2a,b, 4a, and 8b

	2a	2b	4a	8b
chem formula	$C_{30}H_{34}N_4O_2PtS$	$C_{32}H_{38}N_4PtS$	$C_{66}H_{74}Cl_2Cu_2N_8O_4Pt_2S_2$	$C_{36}H_{37}KN_4Pt$
fw	709.76	705.81	847.81	759.89
cryst syst	monoclinic	triclinic	monoclinic	monoclinic
space group	*P*21/*c*	$P\bar{1}$	*P*2/*c*	*P*21/*c*
a [Å]	16.9605(13)	7.8393(14)	24.8131(13)	12.5793(12)
b [Å]	7.6043(12)	13.7453(17)	15.2421(12)	9.2999(11)
c [Å]	22.6425(15)	14.5500(17)	17.6737(15)	28.4841(15)
α [deg]	90	94.905(12)	90	90
β [deg]	92.823(11)	97.696(12)	96.919(13)	92.192(11)
γ [deg]	90	97.360(13)	90 deg	90
V [Å^3]	2916.7(5)	1532.5(4)	6635.6(8)	3329.8(5)
Z	4	2	8	4
D_{calcd} [g cm]	1.616	1.530	1.697	1.516
F(000)	1408	704	3352	1512
μ [mm]	4.915	4.672	5.032	4.368
temp [K]	220(2)	220(2)	220(2)	220(2)
wavelength [Å]	0.71070	0.71070	0.71070	0.71070
no. of measd rflns	10 229	11 179	25 361	11 901
no. of unique rflns	6516	6719	13 371	7439
no. of data/restraints/ params	6516/0/351	6719/0/353	13 371/0/793	7439/0/387
$R(F)$ ($I > 2\sigma(I)$)	0.0433	0.0501	0.0704	0.0412
$wR(F^2)$ ($I > 2\sigma(I)$)	0.1083	0.1182	0.1623	0.1098
GOF	1.018	1.095	1.080	1.036

Table 2. Crystallographic Data for Compounds 9b and 10a,b

	9b	10a	10b
chem formula	$C_{44}H_{49}CuN_8Pt$	$C_{68}H_{66}Cu_2N_8O_4Pt_2$	$C_{78}H_{86}Cu_2N_8O_3Pt_2$
fw	948.54	1576.55	1700.81
cryst syst	triclinic	triclinic	monoclinic
space group	$P\bar{1}$	$P\bar{1}$	*P*21/*c*
a [Å]	12.5439(12)	11.3102(12)	19.7025(13)
b [Å]	12.6310(12)	16.5428(13)	13.3495(12)
c [Å]	14.1299(13)	18.7782(13)	28.314(2)
α [deg]	69.921(12)	112.169(11)	90
β [deg]	85.038(11)	95.433(10)	108.050(11)
γ [deg]	89.992(10)	108.142(11)	90
V [Å^3]	2093.8(3)	3000.8(6)	7080.7(10)
Z	2	2	4
D_{calcd} [g cm]	1.505	1.745	1.595
F(000)	952	1552	3392
μ [mm]	3.885	5.403	4.585
temp [K]	220(2)	220(2)	220(2)
wavelength [Å]	0.71070	0.71070	0.71070
no. of measd rflns	16 067	24 103	27 193
no. of unique rflns	9582	13 645	16 238
no. of data/restraints/ params	9582/0/499	13 645/0/768	16 238/0/853
$R(F)$ ($I > 2\sigma(I)$)	0.0436	0.0543	0.0419
$wR(F^2)$ ($I > 2\sigma(I)$)	0.1090	0.1365	0.0952
GOF	1.034	1.026	0.987

in vacuo to yield the product as a white powder (751 mg, 78%). An analytically pure sample was obtained by vapor diffusion of pentane into a solution of **1b** in dichloromethane. Mp: 228−229 °C. ^{1}H NMR (DMSO-d_6, 300 MHz): δ 13.61 (s, 1H, NH) 7.06 (d, ^3J(H−H) = 7.5 Hz, 4H, ArH^{3,5}), 6.88 (t, ^3J(H−H) = 7.4 Hz, 2H, ArH^4), 2.69 (s, 3H, Pz-CH$_3$), 2.05 (s, 6H, ArN=C(CH$_3$)-Pz), 1.98 (s, 12H, ArCH$_3$). ^{13}C NMR (DMSO-d_6, 300 MHz): δ 162.8 (C=NAr), 158.1 (C=NAr), 148.9 (C^{Ar}), 148.5 (C^{Ar}), 147.6 (C^{Ar}), 137.6 (C^{Ar}), 127.5 (C^{Ar}), 124.7 (C^{Ar}), 124.5 (C^{Ar}), 122.5 (C^{Ar}), 122.1 (C^{Ar}), 116.4 (C^{Ar}), 18.6 (N=CCH$_3$), 18.0 (N=CCH$_3$), 17.0 (C=NArCH$_3$), 11.4 (Pz-CH$_3$). ESI-MS (DCM), positive ion scan: *m*/*z* 373 ([M + H]$^+$). Anal. Calcd for $C_{24}H_{28}N_4$: C 77.38, H 7.58, N 15.04. Found: C 77.09, H 7.55, N 15.03.

Complex Syntheses. *cis*-PtPh$_2$(SMe$_2$)$_2$. A solution of phenyllithium in dibutyl ether (∼2 M, not titrated, 40 mL, 80 mmol) was added at 0 °C to a suspension of finely powdered PtCl$_2$(SMe$_2$)$_2$ (*cis*/*trans* mixture, 2.2 g, 5.6 mmol) in diethyl ether (80 mL), and the resulting beige suspension was stirred for 3.5 h. All workup was performed at 0 °C under argon. Then 40 mL of cooled, N_2-purged water was slowly added. The phases were separated, and the water phase was extracted with dichloromethane (4 × 20 mL). The combined organic phases were dried over $MgSO_4$, treated with a small quantity of activated charcoal, filtered, and evaporated *in vacuo*. The beige residue was dissolved in a mixture of dichloromethane (7 mL) and Me_2S (0.5 mL), and hexane (20 mL) was added until precipitation started. Storage overnight at −20 °C, filtration, washing with hexane (3 × 2 mL), and drying *in vacuo* yielded the product as a beige microcrystalline solid (1.86 g). Concentration of the combined mother liquor and washings and storage overnight at −20 °C yielded an additional crop as a beige solid (0.51 g). Total yield: 2.37 g, 89%. Mp: ≥133 °C (dec) {lit. 100 °C[8]}. ^{1}H NMR ($CDCl_3$, 300 MHz): δ 7.37 (dd, ^3J(H−H) = 7.9 Hz, ^5J(H−H) = 1.4 Hz, ^3J(^{195}Pt−H) = 72.1 Hz, 4H, PtArH^{2,6}) 7.00−6.86 (m, 4H, PtArH^{3,5}), 6.80−6.73 (m, 2H, PtArH^4), 2.11 (s, ^3J(^{195}Pt−H) = 23.6 Hz, SCH$_3$). Anal. Calcd for $C_{16}H_{22}S_2Pt$: C, 40.58, H, 4.68. Found: C, 40.52, H, 4.74.

***trans*-(bmimp)PtPh(SMe$_2$) (*trans*-2a).** A mixture of bmimpH (146 mg, 0.39 mmol) and *cis*-PtPh$_2$(SMe$_2$)$_2$ (183 mg, 0.39 mmol) in 6 mL of dichloromethane was stirred for 3.5 h. The resulting orange solution was filtered and vapor diffused with hexane. After 6 days, the mother solution was decanted, and the yellow crystals were washed with hexane (3 × 3 mL) and dried *in vacuo* (210 mg, 77%). Mp: ≥185 °C (dec). ^{1}H NMR (CD_2Cl_2, 300 MHz): δ 6.49−7.02 (m, 13H, ArH), 3.80 (s, 3H, OCH$_3$), 3.68 (s, 3H, OCH$_3$),

2.68 (s, 3H, Pz-CH_3), 2.65 (s, $^3J(^{195}Pt-H) = 58.3$ Hz, 6H, SCH_3), 2.34 (s, 3H, ArN=C(CH_3)-Pz), 2.26 (s, 3H, ArN=C(CH_3)-Pz). ^{13}C NMR (CD_2Cl_2, 75 MHz): δ 172.7 (C=NAr), 164.6(C=NAr), 157.5 (C^{Ar}), 155.6 (C^{Ar}), 151.1 (C^{Ar}), 150.6 (C^{Ar}), 145.5 (C^{Ar}), 142.0 (C^{Ar}), 139.4 (C^{Ar}), 137.6 (C^{Ar}), 126.6 (C^{Ar}), 125.5 (C^{Ar}), 122.1 (C^{Ar}), 121.6 (C^{Ar}), 121.0 (C^{Ar}), 114.3 (C^{Ar}), 113.4 (C^{Ar}), 55.8 (OCH_3), 24.4 (SCH_3), 18.7 (N=CCH_3), 18.5 (N=CCH_3), 11.4 (Pz-CH_3). ESI-MS (DCM), positive ion scan: *m/z* 710 ($[M + H]^+$). MS/MS (+710): *m/z* 648 (weak, $-$ SMe_2), 632 ($-$ C_6H_6), 570 ($-$ $SMe_2 - C_6H_6$), 588 (weak, $-$ $SMe_2 - C_6H_6 + H_2O$), 598 ($-$ $SMe_2 - C_6H_6 + N_2$). Anal. Calcd for $C_{30}H_{34}N_4O_2SPt$: C 50.77, H 4.83, N 7.89. Found: C 50.99, H 4.89, N 7.87. Crystals suitable for X-ray analysis were obtained by vapor diffusion of hexane into a solution of *trans*-**2a** in 1:1 DCM/hexane at 4 °C.

***trans*-(bdmimp)PtPh(SMe$_2$) (*trans*-2b).** A solution of bdmimpH (150 mg, 0.40 mmol) and *cis*-$PtPh_2(SMe_2)_2$ (190 mg, 0.40 mmol) in dichloromethane (7 mL) was stirred for 66 h. The solution was then concentrated to 2 mL, hexane (10 mL) was added, and the mixture was stirred for 2 h. The pale yellow precipitate was collected by filtration, washed with pentane, and dried *in vacuo*. Concentration of the combined mother solution and washings to 5 mL yielded a second crop of product. Pale yellow powder, 223 mg (79%). Mp: ≥230 °C (dec). ^1H NMR (CD_2Cl_2, 300 MHz): δ 7.05 (d, $^3J(H-H) = 7.5$ Hz, 2H,C=NAr$H^{3,5}$), 6.97−6.90 (m, 2H, PtArH), 6.87 (t, $^3J(H-H) = 7.5$ Hz, 1H, C=NArH^4), 6.79 ("s", 3H, C=NAr$H^{3,4,5}$), 6.62−6.50 (m, 3H, PtArH), 2.75 (s, 3H, Pz-CH_3), 2.62 (s, $^3J(^{195}Pt-H) = 59.3$ Hz, 6H, SCH_3), 2.164 (s, 3H, ArN=C(CH_3)-Pz), 2.159 (s, 6H, C=NArCH_3) 2.14 (s, 3H, ArN=C(CH_3)-Pz), 2.06 (s, 6H, C=NArCH_3). ^{13}C NMR (CD_2Cl_2, 75 MHz): δ 172.5 (C=NAr), 164.0 (C=NAr), 150.7 (C^{Ar}), 150.2 (C^{Ar}), 149.9 (C^{Ar}), 144.0 (C^{Ar}), 140.4 (C^{Ar}), 136.7 (C^{Ar}), 131.0 (C^{Ar}), 127.8 (C^{Ar}), 127.7 (C^{Ar}), 126.3 (C^{Ar}), 126.2 (C^{Ar}), 125.9 (C^{Ar}), 122.3 (C^{Ar}), 122.2 (C^{Ar}), 121.7 (C^{Ar}), 24.3 (SCH_3), 18.7 (N=CCH_3/ArCH_3), 18.3 (N=CCH_3/ArCH_3), 17.4 (N=CCH_3/ArCH_3), 11.7 (Pz-CH_3). ESI-MS (DCM), positive ion scan: *m/z* 706 ($[M + H]^+$). MS/MS (+706): *m/z* 628 ($-$ C_6H_6), 566 ($-$ $C_6H_6 - SMe_2$), 594 (weak, $-$ $C_6H_6 - SMe_2 + N_2$). Anal. Calcd for $C_{32}H_{38}N_4SPt$: C 54.45, H 5.43, N 7.94. Found: C 54.56, H 5.31, N 7.86. Crystals suitable for X-ray analysis were obtained by vapor diffusion of hexane into a solution of *trans*-**2b** in 1:1 dichloromethane/hexane at 4 °C.

***cis*-(bmimp)PtMe(SMe$_2$) (*cis*-3a).** $Pt_2(CH_3)_4(\mu\text{-}Me_2S)_2$ (100 mg, 0.17 mmol) was added as a solid to a suspension of bmimpH (131 mg, 0.35 mmol) in dichloromethane (20 mL), causing complete dissolution and the appearance of a yellow color, together with gas (methane) evolution. The mixture was stirred for 1 h, after which a thin precipitate was removed by filtration over Celite. The product was precipitated by concentration of the solution to 5 mL followed by addition of diethyl ether (15 mL) and stirring for 10 min. Filtration, washing with diethyl ether (3 × 2 mL), and drying *in vacuo* yielded the product as a pale yellow solid (90 mg, 40%). Mp: ≥230 °C (dec). ^1H NMR (CD_2Cl_2, 300 MHz): δ 7.04−6.82 (m, 3H, ArH), 6.79−6.70 (m, 1H, ArH), 3.84 (s, 3H, OCH_3), 3.80 (s, 3H, OCH_3), 2.64 (s, 3H, Pz-CH_3), 2.32 (s, 3H, ArN=C(CH_3)-Pz), 2.16 (s, 3H, ArN=C(CH_3)-Pz), 2.16 (s, $^3J(^{195}Pt-H) = 50.1$ Hz, 6H, S(CH_3)), 1.16 (s, $^2J(^{195}Pt-H) = 80.3$ Hz, 3H, PtCH_3). The two signals at δ 2.16 can be resolved by addition of about 10% C_6D_6 to the sample. ^{13}C NMR (CD_2Cl_2, 75 MHz): δ 169.1 (C=NAr), 165.2 (C=NAr), 158.0 (C^{Ar}), 155.8 (C^{Ar}), 152.3 (C^{Ar}), 150.1 (C^{Ar}), 145.8 (C^{Ar}), 140.5 (C^{Ar}), 124.4 (C^{Ar}), 121.1 (C^{Ar}), 121.0 (C^{Ar}), 114.6 (C^{Ar}), 114.4 (C^{Ar}), 55.79 (OCH_3), 55.75 (OCH_3), 21.5 (SCH_3), 18.4 (N=CCH_3), 18.1 (N=CCH_3), 11.2 (Pz-CH_3, -14.1 ($^1J(^{195}Pt-C) = 726$ Hz, PtCH_3). ESI-MS (DCM), positive ion scan: *m/z* 648 ($[M + H]^+$). MS/MS (+648): *m/z* 632 ($-$ CH_4), 570 ($-$ $CH_4 - SMe_2$), 598 ($-$ $CH_4 - SMe_2 + N_2$). Anal. Calcd for $C_{25}H_{32}N_4O_2SPt$: C 46.36, H 4.98, N 8.65. Found: C 46.45, H 4.96, N 8.54. The stereochemistry was assigned from the ^1H NMR spectrum on the basis of the shielding of the Pt−S(CH_3)$_2$ signal by the *p*-methoxyphenyl group and the $^{195}Pt-H$ coupling constants of the Pt−S(CH_3)$_2$ and Pt−CH_3 signals.[21]

***trans*-(bmimp)PtMe(SMe$_2$) (*trans*-3a).** A mixture of $Pt_2(CH_3)_4(\mu\text{-}Me_2S)_2$ (175 mg, 0.30 mmol) and bmimpH (230 mg, 0.60 mmol) in toluene (4 mL) was stirred for 15 h, yielding an orange suspension. After filtration and washing with toluene (3 × 2 mL), the yellow solid was dissolved in dichloromethane (6 mL), precipitated with diethyl ether (12 mL), filtered, washed with diethyl ether, and dried *in vacuo* to yield *cis*-**3a** (110 mg, 29%). Toluene was evaporated from the liquid phase, and the residue was dissolved in dichloromethane (5 mL). Addition of diethyl ether (10 mL) and concentration *in vacuo* caused the precipitation of *trans*-**3a** as a yellow solid, which was washed with diethyl ether and dried *in vacuo* (32 mg, 8%). An analytically pure sample was obtained by vapor diffusion of hexane into a tetrahydrofuran solution of *trans*-**3a**. Mp: ≥200 °C (dec). ^1H NMR (CD_2Cl_2, 300 MHz): δ 7.05−6.85 (m, 3H, Ar*H*), 6.78−6.72 (m, 1H, Ar*H*), 3.84 (s, 3H, OCH_3), 3.80 (s, 3H, OCH_3), 2.78 (s, $^3J(^{195}Pt-H) = 57.1$ Hz, 6H, SCH_3), 2.65 (s, 3H, Pz-CH_3), 2.33 (s, 3H, ArN=C(CH_3)-Pz), 2.22 (s, 3H, ArN=C(CH_3)-Pz), 0.07 (s, $^2J(^{195}Pt-H) = 69.5$ Hz, 3H, PtCH_3). ^{13}C NMR (CD_2Cl_2, 75 MHz): δ 173.5 (C=NAr), 165.0 (C=NAr), 158.1 (C^{Ar}), 155.9 (C^{Ar}), 150.9 (C^{Ar}), 150.4 (C^{Ar}), 145.8 (C^{Ar}), 139.5 (C^{Ar}), 125.5 (C^{Ar}), 121.3 (C^{Ar}), 121.2 (C^{Ar}), 114.4 (C^{Ar}), 114.2 (C^{Ar}), 55.8 (OCH_3), 24.1 (SCH_3), 18.7 (N=CCH_3), 18.4 (N=CCH_3), 11.4 (Pz-CH_3), -13.0 ($^1J(^{195}Pt-C) = 685$ Hz, PtCH_3). ESI-MS (DCM), positive ion scan: *m/z* 648 ($[M + H]^+$). MS/MS (+648): *m/z* 632 ($-$ CH_4), 604 (weak, $-$ $SMe_2 + H_2O$), 598 ($-$ $CH_4 - SMe_2 + N_2$), 588 (weak, $-$ $CH_4 - SMe_2 + H_2O$), 570 ($-$ $CH_4 - SMe_2$). Anal. Calcd for $C_{25}H_{32}N_4O_2SPt$: C 46.36, H 4.98, N 8.65. Found: C 46.51, H 5.10, N 8.54.

***cis*-(bdmimp)PtMe(SMe$_2$) (*cis*-3b).** A solution of bdmimpH (129 mg, 0.35 mmol) in dichloromethane (15 mL) was added over 15 min to a solution of $Pt_2(CH_3)_4(\mu\text{-}Me_2S)_2$ (100 mg, 0.17 mmol) at 0 °C, causing a gradual color change from colorless to yellow. The solution was stirred for 35 min, then allowed to slowly warm to room temperature and stirred for 2 h. The solvent was evaporated, and the yellow residue was thoroughly washed with hexane and purified by column chromatography over neutral alumina (15 g), using a 1:1 hexane/dichloromethane mixture as eluent. Evaporation of the solvent and drying *in vacuo* afforded the product as a yellow solid (104 mg, 46%). An analytically pure sample was obtained by vapor diffusion of hexane into a dichloromethane solution of *cis*-**3b**. Mp: ≥194 °C (dec). ^1H NMR (CD_2Cl_2, 300 MHz): δ 7.21−6.99 (m, 5H, ArH), 6.86 ("t", $^3J(H-H) = 7.5$ Hz, 1H, ArH^4), 2.74 (s, 3H, Pz-CH_3), 2.22 (s, 6H, C=NArCH_3), 2.16 (s, 3H, ArN=C(CH_3)-Pz), 2.11 (s, $^3J(^{195}Pt-H) = 50.5$ Hz, 6H, SCH_3), 2.062 (s, 3H, ArN=C(CH_3)-Pz), 2.057 (s, 6H, C=NArCH_3), 1.18 (s, $^2J(^{195}Pt-H) = 79.9$ Hz, 3H, PtCH_3). ^{13}C NMR (CD_2Cl_2, 75 MHz): δ 168.8 (C=NAr), 164.6 (C=NAr), 151.9 (C^{Ar}), 150.2 (C^{Ar}), 149.7 (C^{Ar}), 144.8 (C^{Ar}), 130.8 (C^{Ar}), 128.4 (C^{Ar}), 128.0 (C^{Ar}), 126.3 (C^{Ar}), 126.1 (C^{Ar}), 122.3 (C^{Ar}), 121.1 (C^{Ar}), 21.6 (SCH_3), 18.6 (N=CCH_3), 18.3 (C=NArCH_3), 17.9 (C=NArCH_3), 17.3 (N=CCH_3), -12.8 ($^1J(^{195}Pt-C) = 729$ Hz, PtCH_3). ESI-MS (CH_2Cl_2), positive ion scan: *m/z* 644 ($[M + H]^+$). MS/MS (+644): *m/z* 628 ($-$ CH_4), 566 ($-$ $CH_4 - SMe_2$). Anal. Calcd for $C_{27}H_{36}N_4SPt$: C 50.38, H 5.64, N 8.70. Found: C 50.57, H 5.73, N 8.58.

(88) Watson, S. C.; Eastham, J. F. *J. Organomet. Chem.* **1967**, *9*, 165–168.
(89) Wolff, L. *Liebigs Ann. Chem.* **1902**, *325*, 134–195.
(90) Wollf, L. *Liebigs Ann. Chem.* **1912**, *394*, 59–68.
(91) Hill, G. S.; Irwin, M. J.; Levy, C. J.; Rendina, L. M.; Puddephatt, R. J. *Inorg. Synth.* **1998**, *32*, 149–152.
(92) Rashidi, M.; Fakhroeian, Z.; Puddephatt, R. J. *J. Organomet. Chem.* **1990**, *406*, 261–267.

{[*trans*-(bmimp)PtPh(SMe$_2$)]$_2$Cu}{CuCl$_2$} (4a). CuCl (16 mg, 162 μmol) was added to a yellow solution of *trans*-**2a** (28 mg, 39 μmol) in CD_2Cl_2 (0.7 mL), causing an immediate color change to bright red. The mixture was stirred for 10 min and filtered into a Young-type NMR tube, where the product was characterized by ^{1}H and ^{13}C NMR. The solvent was then evaporated *in vacuo*, and the residue was dissolved in benzene (1 mL) and stored at 4 °C for 5 days. Filtration, washing with benzene (2 × 0.5 mL), and drying *in vacuo* yielded the product as dark red microcrystals (17 mg, 56%). Mp: ≥180 °C (dec). ^{1}H NMR (CD_2Cl_2, 300 MHz): δ 7.09−6.89 (m, 2H, br Pt satelites, PtArH), 6.88 ("s", 4H, NAr$H^{2,3,5,6}$), 6.72−6.50 (m, 7H, ArH), 3.81 (s, 3H, OCH_3), 3.68 (s, 3H, OCH_3), 2.59 (s, 3H, Pz-CH_3), 2.35 (s, 3H, ArN=C(CH_3)-Pz), 2.29 (s, 3H, ArN=C(CH_3)-Pz), 2.05 (s, $^3J(^{195}Pt-H)$ = 58.7 Hz, 6H, SCH_3). ^{13}C NMR (CD_2Cl_2, 75 MHz): δ 173.3 (C=NAr), 163.0 (C=NAr), 157.8 (C^{Ar}), 157.2 (C^{Ar}), 151.2 (C^{Ar}), 150.5 (C^{Ar}), 143.1 (C^{Ar}), 141.0 (C^{Ar}), 138.8 (C^{Ar}), 136.3 (C^{Ar}), 127.1 (C^{Ar}), 124.8 (C^{Ar}), 123.1 (C^{Ar}), 122.6 (C^{Ar}), 121.9 (C^{Ar}), 114.3 (C^{Ar}), 113.6 (C^{Ar}), 55.82 (OCH_3), 55.79 (OCH_3), 23.6 (SCH_3), 19.7 (N=CCH_3), 19.6 (N=CCH_3), 11.6 (Pz-CH_3). ESI-MS (CH_2Cl_2), positive ion scan: *m*/*z* 1581 (weak, [M + CuCl]$^+$), 1482 (M+), 773 ([(bmimp)PtPh(SMe$_2$)Cu]$^+$). MS/MS (+1581): *m*/*z*1519 (− SMe$_2$), 871 (weak, − [(bmimp)PtMe(SMe$_2$)]), 773 (− {[(bmimp)PtMe(SMe$_2$)]CuCl}). MS/MS (+1482): *m*/*z* 1420 (− SMe$_2$), 1358 (− 2 SMe$_2$), 1280 (− 2 SMe$_2$ − C_6H_6), 1009 (weak, [(bmimp)$_2$PtCu]+), 773 (− [(bmimp)PtPh(SMe$_2$)]). Negative ion scan: *m*/*z* 135 ([$CuCl_2$]−). Anal. Calcd for $C_{60}H_{68}N_8O_4S_2Cl_2Cu_2Pt_2$: C 44.55, H 4.24, N 6.93. Found: C 44.65, H 4.12, N 6.77. Crystals suitable for X-ray analysis were obtained from a freshly prepared solution of **4a** in benzene.

{[*cis*-(bmimp)PtMe(SMe$_2$)]$_2$Cu}{CuCl$_2$} (5a). An excess of CuCl was added to a suspension of *cis*-**3a** (40 mg, 62 μmol) in CD_2Cl_2 (0.7 mL), and the resulting dark red mixture was stirred for 5 min and filtered into a Young-type NMR tube. ^{1}H NMR (CD_2Cl_2, 300 MHz): δ 7.01 (d, ^3J(H−H) = 9.1 Hz, 4H, NAr$H^{2,6/3,5}$), 6.90 (d, ^3J(H−H) = 8.9 Hz, 4H, NAr$H^{3,5/2,6}$), 6.82 ("s", 4H, NAr$H^{2,3,5,6}$), 3.85 (s, 6H, OCH_3), 3.79 (s, 6H, OCH_3), 2.57 (s, 6H, Pz-CH_3), 2.29 (s, 6H, ArN=C(CH_3)-Pz), 2.19 (s, 3H, ArN=C(CH_3)-Pz), 2.11 (s, $^4J(^{195}Pt-H)$ = 54 Hz, 12H, SCH_3) 1.08 (s, $^3J(^{195}Pt-H)$ = 77.4 Hz, $PtCH_3$). ^{13}C NMR (CD_2Cl_2, 75 MHz): δ 168.8 (C=NAr), 162.5 (C=NAr), 158.3 (C^{Ar}), 157.1 (C^{Ar}), 153.0 (C^{Ar}), 150.0 (C^{Ar}), 141.7 (C^{Ar}), 139.7 (C^{Ar}), 124.1 (C^{Ar}), 123.2 (C^{Ar}), 121.2 (C^{Ar}), 114.8 (C^{Ar}), 114.3 (C^{Ar}), 55.9 (OCH_3), 21.6 (SCH_3), 19.3 (N=CCH_3), 19.1 (N=CCH_3), 11.6 (Pz-CH_3), −12.5 ($PtCH_3$). ESI-MS (CH_2Cl_2), positive ion scan: *m*/*z* 1358 (M+). MS/MS (+1358): *m*/*z* 1342 (− CH_4), 1296 (− SMe$_2$), 1280 (− CH_4 − SMe$_2$), 1264 (− 2 CH_4 − SMe$_2$), 1218 (− CH_4 − 2 SMe$_2$), 1202 (− 2 CH_4 − 2 SMe$_2$), 1154 ([(bmimp)$_2$Pt$_2$$CH_3$]$^+$ 1140 ([(bmimp)$_2$Pt$_2$]$^+$), 1009 ([(bmimp)$_2$PtCu]$^+$), 711 (weak, (− [(bmimp)PtMe(SMe$_2$)]). Negative ion scan: *m*/*z* 135 ([$CuCl_2$]$^-$).

[*trans*-(bdmimp)PtPh(SMe$_2$)]·CuCl (4b). An excess of CuCl was added to a suspension of *trans*-**2b** in CD_2Cl_2 (0.7 mL), and the resulting dark red mixture was stirred for 5 min and filtered into a Young-type NMR tube. ^{1}H NMR (CD_2Cl_2, 300 MHz): δ 7.24−6.86 (br m, 5H, Ar*H*), 6.79 (br, 3H, Ar*H*), 6.61 (br, 3H, Ar*H*), 2.60 (s, 3H, OCH_3), 2.42−1.80 (br m, ∼23H, CH_3), 1.12 (very br, ∼1H, CH_3). ESI-MS (CH_2Cl_2), positive ion scan: *m*/*z* 1573 ([(bdmimp)PtPh(SMe$_2$)]$_2$$Cu_2Cl^+$), 1474 ([(bdmimp)PtPh(SMe$_2$)]$_2$-Cu$^+$). MS/MS (+1573): *m*/*z* 1511 (− SMe$_2$), 1449 (− 2SMe$_2$), 867 (− [(bdmimp)PtPh(SMe$_2$)]), 805 (− [(bdmimp)PtPh(SMe$_2$)] − SMe$_2$), 769 (weak, [(bdmimp)PtPh(SMe$_2$)] − CuCl), 727 (− [(bdmimp)PtPh(SMe$_2$)] − SMe$_2$ − C_6H_6). MS/MS (+1474): *m*/*z* 1412 (− SMe$_2$), 1334 (weak, − SMe$_2$ − C_6H_6), 1272 (− 2SMe$_2$ − C_6H_6), 1194 (weak, − 2SMe$_2$ − 2C_6H_6), 769 (− [(bdmimp)PtPh(SMe$_2$)]), 707 (− [(bdmimp)PtPh(SMe$_2$)] − SMe$_2$), 691 (− [(bdmimp)PtPh(SMe$_2$)] − C_6H_6), 629 (− [(bdmimp)PtPh(SMe$_2$)] − SMe$_2$ − C_6H_6). Negative ion scan: *m*/*z* 135 ([$CuCl_2$]$^-$), 233 (weak, [Cu_2Cl_3]$^-$).

[*cis*-(bdmimp)PtMe(SMe$_2$)]·CuCl (5b). An excess of CuCl was added to a suspension of *cis*-**3b** (40 mg, 62 μmol) in CD_2Cl_2 (0.7 mL), and the resulting dark red mixture was stirred for 5 min and filtered into a Young-type NMR tube. ^{1}H NMR (CD_2Cl_2, 300 MHz): δ 7.20 ("d", ^3J(H−H) = 7.2 Hz, 4H, NAr$H^{3,5}$), 7.10 (dd, ^3J(H−H) = 8.5 Hz, ^3J(H−H) = 6.4 Hz, 2H, NArH^4), 7.04−6.70 (br m, 6H, NAr$H^{3,4,5}$), 2.58 (s, 6H, Pz-CH_3), 2.34−1.85 (br m, ∼30H, CH_3), 2.20 ("s", ∼12H, CH_3), 2.08 ("s", ∼12H, CH_3), 1.16 (br, ∼6H, CH_3), 0.85 (br, ∼6H, $^3J(^{195}Pt-H) \approx 77$ Hz, PtCH_3). ESI-MS (CH_2Cl_2), positive ion scan: *m*/*z* 1350 ({[(bdmimp)PtMe(SMe$_2$)]$_2$-Cu}$^+$), 707 ({[(bdmimp)PtMe(SMe$_2$)]Cu}$^+$). MS/MS (+1350): *m*/*z* 1334 (weak, − CH_4), 1288 (weak, − SMe$_2$), 1272 (− CH_4 − SMe$_2$), 1194 (weak, − 2 CH_4 − 2 SMe$_2$), 707 (− [(bdmimp)PtMe(SMe$_2$)]), 691 (− [(bdmimp)PtMe(SMe$_2$)] − CH_4), 663 (− [(bdmimp)PtMe(SMe$_2$)] − SMe$_2$ + H_2O), 629 (− [(bdmimp)PtMe(SMe$_2$)] − CH_4 − SMe$_2$). MS/MS (+707): *m*/*z* 691 (− CH_4), 663 (− SMe$_2$ + H_2O), 645 (weak, − SMe$_2$), 629 (− CH_4 − SMe$_2$). Negative ion scan: *m*/*z* 135 ([$CuCl_2$]$^-$), 233 (weak, [Cu_2Cl_3]$^-$).

[(bmimp)PtPh$_2$]$^-$K$^+$ (8a). A mixture of bmimpH (200 mg, 0.53 mmol) and KO^{t}Bu (60 mg, 0.53 mmol) in tetrahydrofuran (5 mL) was stirred for 0.5 h, resulting in a brown solution. The solvent was evaporated *in vacuo*, and dichloromethane (5 mL) was added and evaporated *in vacuo*. This cycle was repeated two times, and dichloromethane (6 mL) was added to the residue. The resulting beige suspension was cooled to 0 °C, and *cis*-PtPh$_2$(SMe$_2$)$_2$ (252 mg, 0.53 mmol) was added. The mixture was allowed to warm to room temperature and stirred for 63 h. Filtration, washing of the solid with dichloromethane (2 × 1 mL), and drying *in vacuo* afforded the product as a yellow powder (270 mg, 67%). An analytically pure sample was obtained by crystallization from acetonitrile. Mp: ≥150 °C (dec). ^{1}H NMR (CD_3CN, 300 MHz): δ 7.41 (dd, ^3J(H−H) = 8.0 Hz, ^5J(H−H) = 1.5 Hz, ^3J(Pt−H) = 73.0 Hz, 2H, PtAr$H^{2,6}$), 6.95 (dd, ^3J(H−H) = 7.9 Hz, ^5J(H−H) = 1.6 Hz, ^3J(Pt−H) = ∼64 Hz, 2H, PtAr$H^{2,6}$), 6.93−6.86 (m, 2H, Ar*H*), 6.81−6.52 (m, 9H, Ar*H*), 6.48−6.33 (m, 3H, Ar*H*), 3.77 (s, 3H, OCH_3), 3.68 (s, 3H, OCH_3), 2.61 (s, 3H, Pz-CH_3), 2.18 (s, 3H, ArN=C(CH_3)-Pz), 2.14 (s, 3H, ArN=C(CH_3)-Pz). ^{13}C NMR (THF-d_8, 75 MHz): δ 167.8 (*C*=NAr), 164.5 (*C*=NAr), 157.8 (C^{Ar}), 156.6 (C^{Ar}), 153.5 (C^{Ar}), 151.7 (C^{Ar}), 150.8 (C^{Ar}), 147.9 (C^{Ar}), 146.3 (C^{Ar}), 141.8 (C^{Ar}), 141.5 (C^{Ar}), 140.0 (C^{Ar}), 126.2 (C^{Ar}), 125.7 (C^{Ar}), 125.6 (C^{Ar}), 121.8 (C^{Ar}), 120.9 (C^{Ar}), 119.8 (C^{Ar}), 114.8 (C^{Ar}), 113.6 (C^{Ar}), 55.7 (O*C*H_3), 19.4 (N=*C*CH_3), 12.2 (Pz-*C*H_3). ESI-MS (MeCN), positive ion scan: *m*/*z* 764 ([M − K^+ + H]$^+$), 1489 ([2 M$^-$ + K^+ + 2H]$^+$). MS/MS (+764): *m*/*z* 608 (− 2 C_6H_6), 626 (− 2 C_6H_6 + H_2O), 636 (− 2 C_6H_6 + N_2), 647 (weak, − 2 C_6H_6 + MeCN), 704 (weak, − C_6H_6 + H_2O), 714 (− C_6H_6 + N_2). MS/MS (+1489): *m*/*z* 764 (− M − H^+). Negative ion scan: *m*/*z* −724 (M^-), −646 ([M − C_6H_6]$^-$), −1488 ([2 M + K]$^-$). MS/MS (−724): *m*/*z* −646 (− C_6H_6). MS/MS (−1488): *m*/*z* −724 (− M − K^+) −646 (− M − K^+ − C_6H_6). Anal. Calcd for $C_{34}H_{33}N_4O_2KPt$: C 53.46, H 4.35, N 7.33. Found: C 53.50, H 4.21, N 7.39.

[(bdmimp)PtPh$_2$]$^-$K$^+$ (8b). A mixture of bdmimpH (200 mg, 0.54 mmol) and KO^{t}Bu (60 mg, 0.53 mmol) in tetrahydrofuran (5 mL) was stirred for 0.5 h, resulting in a brown solution. The solvent was evaporated *in vacuo*, and dichloromethane (5 mL) was added and evaporated in vacuo. This cycle was repeated, and dichloromethane (6 mL) was added to the residue. The resulting off-white suspension was cooled to 0 °C, and *cis*-PtPh$_2$(SMe$_2$)$_2$ (254 mg, 0.54 mmol) was added. The mixture was allowed to warm to room temperature and stirred for 68 h. Filtration, washing of the solid with dichloromethane (2 × 1 mL), and drying *in vacuo* afforded the product as a yellow powder (300 mg, 73%). An analytically pure sample was obtained by vapor diffusion of diethyl ether into an acetonitrile solution of **8b**. Mp: ≥ 230 °C (dec). ^{1}H NMR (CD_3CN, 300

MHz): δ 7.44 (dd, ^3J(H−H) = 8.0 Hz, ^5J(H−H) = 1.5 Hz, ^3J(Pt−H) = 72.9 Hz, 2H, PtArH^{2,6}), 7.11−6.60 (m, 11H, ArH), 6.42−6.26 (m, 3H, ArH), 2.68 (s, 3H, Pz-CH_3), 2.18 (s, 6H, NArCH_3), 2.02 (s, 6H, NArCH_3), 2.00 (s, 3H, ArN=C(CH_3)-Pz), 1.99 (s, 3H, ArN=C(CH_3)-Pz). ^{13}C NMR (CD_3CN, 75 MHz): δ 168.9 (*C*=NAr), 164.9 (*C*=NAr), 152.8 (C^{Ar}), 151.2 (C^{Ar}), 150.7 (C^{Ar}), 150.2 (C^{Ar}), 147.2 (C^{Ar}), 146.7 (C^{Ar}), 140.9 (C^{Ar}), 139.3 (C^{Ar}), 131.0 (C^{Ar}), 128.5 (C^{Ar}), 127.8 (C^{Ar}), 126.8 (C^{Ar}), 126.3 (C^{Ar}), 125.6 (C^{Ar}), 125.2 (C^{Ar}), 122.9 (C^{Ar}), 121.1 (C^{Ar}), 120.3 (C^{Ar}), 120.0 (C^{Ar}), 19.3 (N=CCH_3/ArCH_3), 18.3 (N=CCH_3/ArCH_3), 17.9 (N=CCH_3/ArCH_3), 11.9 (Pz-CH_3). ESI-MS (MeCN), positive ion scan: *m/z* 760 ([M − K$^+$ + H]$^+$), 1481 ([2 M$^-$ + K$^+$ + 2H]$^+$). MS/MS (+760): *m/z* 604 (− 2 C_6H_6). MS/MS (+1481): *m/z* 760 (− M − H$^+$). Negative ion scan: *m/z* −720 (M$^-$), −642 ([M − C_6H_6]$^-$), −1480 ([2 M + K]$^-$). MS/MS (−720): *m/z* −642 (− C_6H_6). MS/MS (−1480): *m/z* −720 (− M − K$^+$) −646 (− M − K$^+$ − C_6H_6). Anal. Calcd for $C_{36}H_{37}N_4OKPt$: C 56.90, H 4.91, N 7.37. Found: C 57.19, H 4.90, N 7.37. Crystals suitable for X-ray diffraction were obtained by vapor diffusion of diethyl ether into an acetonitrile solution of **8b**.

[(bdmimp)PtPh$_2$]Cu(NCMe)$_2$ (9b). A solution of CuCl (3 mg, 30 μmol) in acetonitrile (0.5 mL) was added to a solution of **8b** (20 mg, 26 μmol) in acetonitrile (0.5 mL) and stirred for 1 min. The resulting yellow suspension was immediately filtered, and the yellow solution was stored at −35 °C overnight. The yellow microcrystals that formed during this time were collected by filtration, washed with acetonitrile (3 × 0.1 mL), and suspended in acetonitrile (1 mL). Heating to 50 °C caused complete dissolution, after which the solution was allowed to cool slowly to room temperature. Upon standing, yellow blocks of **9b** suitable for X-ray diffraction were obtained. Further characterization was precluded by the ability of **9b** to lose acetonitrile when exposed to vacuum and to convert to **10b** in solvents other than acetonitrile.

[(bmimp)PtPh$_2$]$_2$Cu$_2$ (10a). A solution of CuCl (69 mg, 0.70 mmol) in acetonitrile (3 mL) was added under stirring to a solution of **8a** (500 mg, 0.65 mmol) in acetonitrile (30 mL), resulting in an immediate color change from yellow to orange followed by the appearance of a yellow solid after 1 min. The yellow suspension was concentrated to about 10 mL and stored at −20 °C overnight. Filtration at −15 °C, washing with precooled acetonitrile (3 × 3 mL), and drying *in vacuo* afforded a yellow solid, which was extracted with benzene (5 + 2 + 2 mL), resulting in a red solution. Solvent was evaporated *in vacuo*, and the brick red residue was dissolved in benzene (7 mL) and vapor diffused with hexane (15 mL) over 12 days. Filtration, washing with hexane (3 × 5 mL), and drying *in vacuo* yielded the product as red needles (452 mg, 88%). Mp: ≥260 °C (dec). ^{1}H NMR (CD_2Cl_2, 300 MHz, 22 °C): δ 8.1−7.0 (v br, 2H, PtAr*H*^{2,6}), 7.0−6.3 (br m, 16H, Ar*H*), 3.78 (s, 3H, OCH_3), 3.68 (s, 3H, OCH_3), 2.54 (br, 3H, Pz-CH_3), 2.21 (br, 6H, ArN=C(CH_3)-Pz). ^{1}H NMR (CD_2Cl_2, 300 MHz, −30 °C), *species A:* δ 7.94 (d, br Pt satellites, ^3J(H−H) = 7.1 Hz, 1H, PtAr*H*$^{2/6}$), 7.1−6.2 (br m, 16H, Ar*H*), 6.02 ("t", ^3J(H−H) = 7.3 Hz, 1H, Ar*H*), 3.74 (s, 3H, OCH_3), 3.69 (s, 3H, OCH_3), 2.56 (s, 3H, Pz-CH_3), 2.26 (s, 3H, ArN=C(CH_3)-Pz) 2.08 (s, 3H, ArN=C(CH_3)-Pz); *species B:* δ 7.90 (d, br Pt satellites, ^3J(H−H) = 7.3 Hz, 1H, PtAr*H*$^{2/6}$), 7.32 (d, br Pt satellites, ^3J(H−H) = 6.4 Hz, 1H, PtAr*H*$^{2/6}$), 7.1−6.2 (br m, 16H, Ar*H*), 3.77 (s, 3H, OCH_3), 3.65 (s, 3H, OCH_3), 2.51 (s, 3H, Pz-CH_3), 2.23 (s, 3H, ArN=C(CH_3)-Pz), 2.17 (s, 3H, ArN=C(CH_3)-Pz). A/B ratio ≈ 4:3. ESI-MS (MeCN), positive ion scan: *m/z* 892 ([((bmimp)PtPh$_2$)Cu(MeCN) + Cu]$^+$), 1639 ({[(bmimp)PtPh$_2$]$_2$Cu$_2$ + Cu}$^+$). MS/MS (+1639): *m/z* 1561 (weak, − C_6H_6), 1483 (− 2 C_6H_6), 1407 (− Ph$_2$ − C_6H_6). MS/MS (+892): *m/z* 851 (− MeCN). Negative ion scan: *m/z* −1512 ({[(bmimp)PtPh$_2$]$_2$Cu}$^-$), −724 ([(bmimp)PtPh$_2$]$^-$). MS/MS (−1512): *m/z* −724 ([(bmimp)PtPh$_2$]$^-$), −646 (weak, [(bmimp)PtPh$_2$ − C_6H_6]$^-$). MS/MS (−724): *m/z* −646 (− C_6H_6). Anal. Calcd for $C_{68}H_{66}N_8O_2Pt_2Cu_2$: C 51.81, H 4.22, N 7.11. Found: C 52.04, H 4.11, N 7.07. Crystals suitable for X-ray diffraction were obtained by vapor diffusion of hexane into a benzene solution of **10a**.

[(bdmimp)PtPh$_2$]$_2$Cu$_2$ (10b). A solution of CuCl (44 mg, 0.44 mmol) in acetonitrile (2 mL) was added under stirring to a solution of **8b** (300 mg, 0.39 mmol) in acetonitrile (10 mL). The resulting yellow suspension was concentrated to 5 mL and stored at −20 °C overnight. Filtration at −10 °C, washing with precooled acetonitrile (3 + 1 + 1 mL), and drying *in vacuo* afforded a yellow solid, which was taken up in benzene (6 mL). The solvent was evaporated *in vacuo*, and the orange residue was extracted with benzene (6 + 1 mL), affording an orange solution, which was vapor diffused with hexane (20 mL) over 7 days. Filtration, washing with hexane (3 × 1 mL), and drying *in vacuo* yielded the product as orange plates containing 2 equiv of benzene (185 mg, 60%). Mp: ≥230 °C (dec). ^{1}H NMR (CD_2Cl_2, 300 MHz): δ 7.77 (d, ^3J(H−H) = 6.9 Hz, ^3J(Pt−H) ≈ 63 Hz, 2H, PtAr*H*^{2,6}), 7.1−6.3 (m, 16H, ArH), 2.54 (s, 3H, Pz-CH_3), 2.21 (s, 3H, NArCH_3/ArN=C(CH_3)-Pz), 2.17 (s, 3H, NArCH_3/ArN=C(CH_3)-Pz), 2.16 (s, 3H, NArCH_3/ArN=C(CH_3)-Pz), 2.11 (s, 3H, NArCH_3/ArN=C(CH_3)-Pz), 2.04 (s, 3H, NArCH_3/ArN=C(CH_3)-Pz), 1.63 (s, 3H, NArCH_3/ArN=C(CH_3)-Pz). ^{13}C NMR (CD_2Cl_2, 75 MHz): δ 169.1 (*C*=NAr), 164.5 (*C*=NAr), 152.1 (C^{Ar}), 149.6 (C^{Ar}), 147.2 (C^{Ar}), 144.8 (C^{Ar}), 144.6 (C^{Ar}), 140.4 (br, C^{Ar}), 137.0 (C^{Ar}), 130.0 (C^{Ar}), 129.8 (C^{Ar}), 128.5 (C^{Ar}), 128.4 (C^{Ar}), 125.7 (C^{Ar}), 125.3 (C^{Ar}), 123.9 (C^{Ar}), 120.8 (C^{Ar}), 120.4 (C^{Ar}), 119.5 (C^{Ar}), 20.6 (N=CCH_3/ArCH_3), 19.6 (N=CCH_3/ArCH_3), 18.8 (N=CCH_3/ArCH_3), 18.6 (N=CCH_3/ArCH_3), 18.5 (N=CCH_3/ArCH_3), 17.8 (N=CCH_3/ArCH_3), 12.3 (Pz-CH_3). ESI-MS (MeCN), positive ion scan: *m/z* 888 ([((bmimp)PtPh$_2$)Cu(MeCN) + Cu]$^+$), 1631 ([(bmimp)-PtPh$_2$]$_2$Cu$_2$ + Cu$^+$). MS/MS (1631): *m/z* 1553 (weak, − C_6H_6), 1475 (− 2C_6H_6), 1399 (− Ph$_2$ − C_6H_6). MS/MS (888): *m/z* 847 (− MeCN). Negative ion scan: *m/z* −1504 ([(bmimp)PtPh$_2$]$_2$-Cu$^-$), −720 ([(bmimp)PtPh$_2$]$^-$). MS/MS (−1504): *m/z* −720 ([(bmimp)PtPh$_2$]$^-$), −642 ([(bmimp)PtPh$_2$ − C_6H_6]$^-$). MS/MS (−720): *m/z* −642 (− C_6H_6). Anal. Calcd for $C_{72}H_{74}N_8Pt_2$-Cu_2·2C_6H_6: C 58.49, H 5.03, N 6.50. Found: C 58.10, H 4.99, N 6.51. Crystals suitable for X-ray diffraction were obtained by vapor diffusion of hexane into a 1,4-dioxane solution of **10b**.

Crystallographic Data. Relevant details about the structure refinements are given in Tables 1 and 2, and selected geometrical parameters are included in the captions of the corresponding figures. Data collection was performed on a Bruker-Nonius Kappa-CCD (graphite monochromator, Mo Kα) at a temperature of 220 K. The structures were solved by direct methods[93] and refined by full-matrix least-squares analysis[94] including an isotropic extinction correction. All non H-atoms were refined anisotropically (H atoms isotropic, whereby H-positions are based on stereochemical considerations).

Acknowledgment. The authors acknowledge support from the Swiss National Science Foundation. We thank T. Michl for the first synthesis of **8a** and Mr. Paul Seiler for the X-ray structure determinations, as well as Dr. Marc-Olivier Ebert for assistance with EXSY-NMR experiments.

(93) Altomare, A.; Burla, M.; Camalli, M.; Cascarano, G.; Giacovazzo, C.; Guagliardi, A.; Moliterni, A.; Polidori, G.; Spagna, R. *J. Appl. Crystallogr.* **1999**, *32*, 115–119.

(94) Sheldrick, G. M. *SHELXL-97*, Program for the Refinement of Crystal Structures; University of Goettingen: Germany, 1997.

Supporting Information Available: ESI-MS and ^{1}H NMR spectra relative to the C−H activation experiments. Variable-temperature ^{1}H NMR data. EXSY spectrum of **4b** ⇄ **6b** and assignment. ESI-MS, ^{1}H and ^{13}C NMR spectra for new compounds. Crystal data in CIF format. This material is available free of charge via the Internet at http://pubs.acs.org.

OM800403Y